HOT WIRE MEASUREMENTS IN A MOMENTUM-CONSERVING AXISYMMETRIC JET

by

DeXiu Peng

A Thesis Submitted to the Faculty
of the Graduate School of State University
of New York at Buffalo in partial fulfillment
of the requirements for the degree of
Master of Science

September 1985

ACKNOWLEDGEMENTS

I would like to express my deep appreciation to my advisor, Dr. William K. George, for guidance, advice and encouragement throughout my graduate studies. I also wish to thank Dr. Steven P. Capp who helped in understanding his dissertation and Mr. Scott Woodward for his special contributions in the laboratory. I also appreciate the help of our secretary Mrs. Eileen Graber who did much to make my graduate studies pleasant and successful. Many thanks are due to all who have helped me with this investigation and my graduate studies.

ABSTRACT

Measurements are reported of extensive hot-wire surveys of an axisymmetric turbulent jet. The jet exit Reynolds number was 9.3×10^4 insuring that the asymptotic jet was fully turbulent. The jet had previously been shown to be momentum-conserving and self-preserving by the laser Doppler anemometer measurements of Capp (1983). Hot wire measurements were carried out at axial distances up to 50 exit diameters.

The hot wire measurements show velocities somewhat higher than those measured by LDA techniques, contrary to results reported previously by a number of researchers. The results are consistent, however, with the well-known sources of error which cause such probes to always measure values which are too high if the flow is turbulent. These results strongly support Capp's allegation that there was a significant problem in the design of the earlier experiments.

TABLE OF CONTENTS

LIST OF FIGURES

NOMENCLATURE

x	=	axial coordinate with respect to virtual origin
x'	=	axial coordinate with respect to jet exit
x_o	=	$x' - x$
r	=	radial coordinate
ω	=	azimuthal coordinate
D	=	jet exit diameter
A	=	jet exit area
U	=	mean axial velocity
U_o	=	jet exist velocity
U_c	=	mean axial velocity of centerline
v	=	mean radial velocity
W	=	mean velocity in aximuthal direction (=0)
u	=	fluctuating axial velocity
v	=	fluctuating radial velocity
w	=	fluctuating velocity in aximuthal direction
η	=	similarity variable ($\eta=r/x$)
$\eta_{1/2}$	=	non-dimensional radial distance at which ($U=U_m/2$)
$f(\eta)$	=	similarity variable defined by equation (2.9)
ρ	=	fluid density
R_t	=	turbulent Reynolds number
M_o	=	rate at which momentum (per unit mass) is added at the source
B_u	=	empirical constant defined by Equation (2.12)

CHAPTER 1

INTRODUCTION

The axisymmetric turbulent incompressible and isothermal jet is an old and a new subject for turbulent researchers because it can be easily generated in the laboratory and most turbulence behavior can be observed. Many measurements with Pitot-tubes, constant temperature anemometers (CTA) and laser Doppler anenometers (LDA) have been reported, eg. Reichart (1942), Corrsin (1943), Hinze and Kistler (1949), Townsend (1956), Sami (1967), Wygnanski and Fiedler (1969) Rodi (1975) and Capp (1983).

In the high turbulence intensity flows Pitot tubes and hot-wires have some serious problems. The Pitot tube and hot-wire response is always higher than the true value because of the effect of the fluctuating velocities. When the turbulent flow changes direction the hot-wire will get the same answer if the magnitude of the normal velocity to the wire is the same since the wire cannot distinguish direction. It is possible to show that these errors are always positive. However, in Wygnanski and Fiedler's jet measurements, the velocity profile was lower than in the LDA data of Capp (1983). Moreover, momentum was not conserved.

In those experiments, the nozzle was placed in the middle of a large room in a screen cage 7.5 ft high and 8 ft. wide, and open on the far side. Capp argued that this cage was not big enough and that the back flow caused by the turbulent entrainment influenced the jet flow shape. Capp's and our experiments were set in a big cage (15 ft. high, 15.2 ft. wide, 50.4 ft. long) and the traversing system was entirely under minicomputer control so that the data could be taken automatically with no one inside to influence the measurements.

The purpose of our experiment was to prove whether, in fact, the hot-wire data is higher than the LDA method as expected and the earlier results represent a problem in the facility, or whether additional sources of error are necessary to explain the discrepancies.

CHAPTER 2

THE EQUATION OF MOTION FOR THE TURBULENT AXISYMMETRIC JET

2.1 In the Infinite Environment

The axisymmetric turbulent jet in an infinite environment can be analyzed by reducing the Navier-Stokes equations. Figure 2-1 shows the coordinate system and nomenclature of the axisymmetric turbulent jet. The axial coordinate is x, and the radial coordinate is r. All derivatives with respect to the azimuthal coordinate are assumed zero as is the azimuthal component of mean velocity. The virtual origin is the location of an ideal source, the axial coordinate with respect to this point being defined as x.

For an isothermal Newtonian incompressible fluid the Reynolds decomposition can be performed on the momentum and continuity equations. For an infinite environment, the averaged continuity equation is

$$\frac{\partial U}{\partial x} + \frac{1}{r}\frac{\partial (rV)}{\partial r} = 0 \qquad (2.1)$$

For high Reynolds number, the viscous terms in the remaining equations of motion can be ignored. The axial component of the averaged momentum equation is

$$U\frac{\partial U}{\partial x} + V\frac{\partial U}{\partial r} = -\frac{1}{\rho}\frac{\partial P}{\partial x} - \frac{1}{r}\frac{\partial (\overline{ruv})}{\partial r} + \frac{\partial \overline{u^2}}{\partial x} \qquad (2.2)$$

The viscous terms in the radial equation are also ignored. This equation is further simplified by an order of magnitude analysis (v. Capp 1983) to yield

$$0 = -\frac{1}{\rho}\frac{\partial P}{\partial r} - \frac{1}{r}\frac{\partial (\overline{rv^2})}{\partial r} - \frac{\overline{w^2}}{r} \qquad (2.3)$$

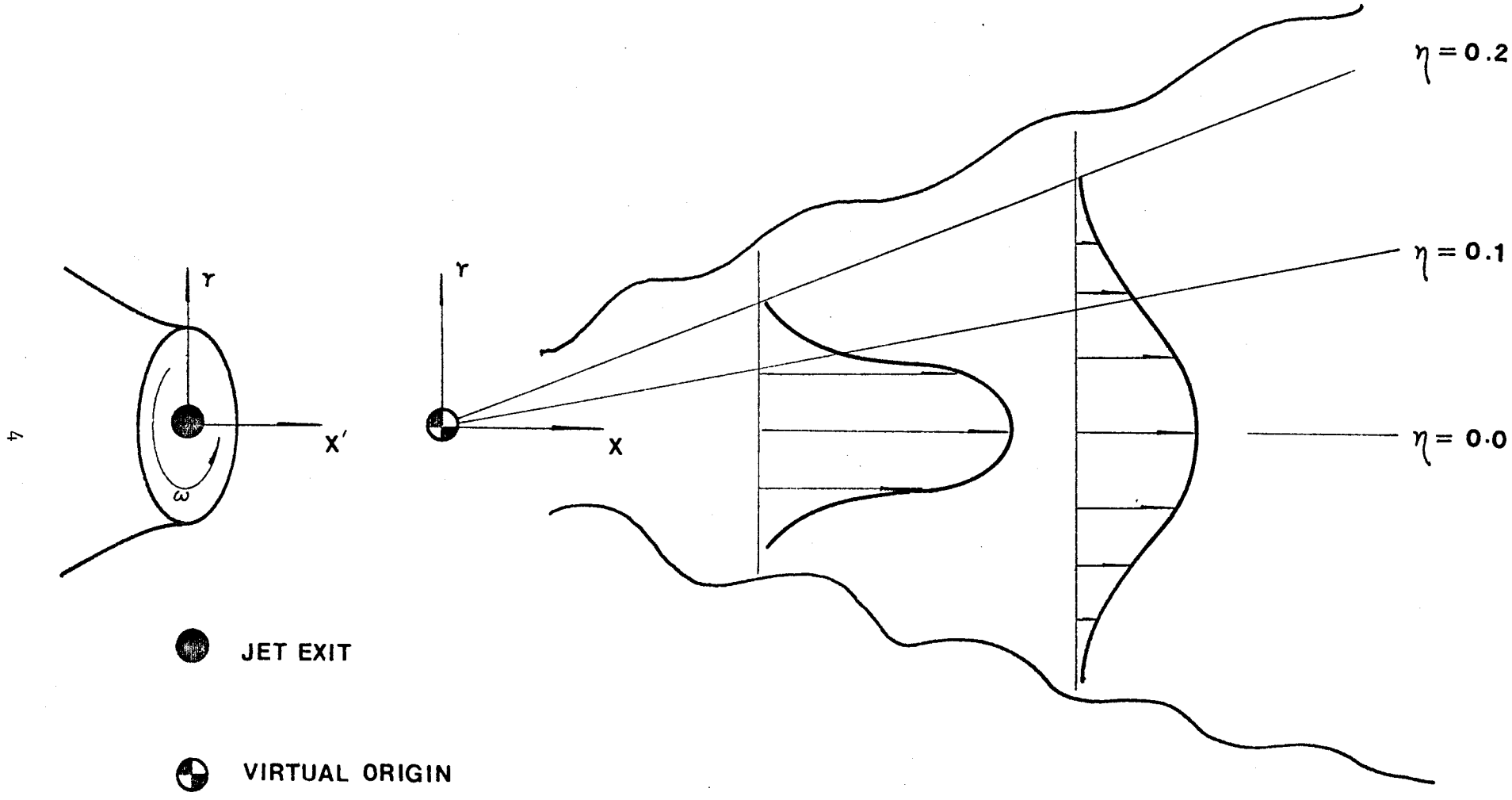

FIGURE : 2 – 1

COORDINATE SYSTEM FOR AXISYMMETRIC JET

Integrating this equation and substituting into equation (2.2) yields

$$U\frac{\partial U}{\partial x} + V\frac{\partial U}{\partial r} = \frac{-1}{r}\frac{\partial(r\overline{uv})}{\partial r} + \frac{\partial}{\partial x}(\overline{v^2}-\overline{u^2}) + \frac{\partial}{\partial x}\int_r^\infty \frac{\overline{w^2}-\overline{v^2}}{r'}\,dr' \quad (2.4)$$

If the second order term is dropped the simpler form is

$$U\frac{\partial U}{\partial x} + V\frac{\partial U}{\partial r} = -\frac{1}{r}\frac{\partial(r\overline{uv})}{\partial r} \quad (2.5)$$

The boundary conditions are as follows:

$U(x,r) = 0$ as r approaches infinity

$\overline{uv}(x,r) = 0$ at r=0 and as r approaches infinity

$V(x,r) = 0$ at r=0 and as r approaches infinity (2.6)

The equation set requires one additional boundary condition. The continuity equation and axial momentum equation can be combined to yield an integral constraint. This constraint requires that the momentum swept past any cross-section is constant for all axial positions. The final boundary condition can be evaluated at the jet exit to yield

$$M_o = 2\pi\int_o^\infty U^2\,r\,dr \quad (2.7)$$

The constant term M_o is called the kinematic momentum. If the velocity is uniform at the exit

$$M_o = (\pi D^2/4)U_o^2 = A_oU_o^2 \quad (2.8)$$

By directly integrating the momentum equations across the jet, Capp was able to show that

$$M_o = \int_o^\infty (U^2 + \overline{u^2} - \frac{\overline{u^2}+\overline{\omega^2}}{2})\,2\pi r\,dr \quad (2.9)$$

If the jet can be said to be momentum conserving, the integral must be constant at any cross section.

2.2: The Similarity Analysis

The equations of motion can be further simplified by mapping the system of equations into similarity variables. These are:

$$U = M_o^{1/2}/x\ f(\eta) \qquad \text{for} \qquad \eta = r/x \tag{2.10}$$

$$\overline{uv} = M_o/x^2 s(\eta) \tag{2.11}$$

U_c is the centerline velocity

$$U_c = B_m\ M_o^{1/2}/x \qquad \text{for} \qquad B_m = f(\eta=0) \tag{2.12}$$

or

$$U_o/U_c = 1/B_u\ [x'/D - xo/D] = 1/B_u\ (x/D) \tag{2.13}$$

where

$$B_u = (\pi/4)\ 0.5\ B_m$$

The continuity equation can be used to determine the radial velocity as a function of the axial velocity.

$$V = \frac{M_o^{1/2}}{x}\ k(\eta) = \frac{M_o^{1/2}}{x}\ (\eta f - \frac{1}{\eta}\int_o^\eta \eta f d\eta) \tag{2.14}$$

The resultant momentum equation is an ordinary differential equation given by

$$f^2 + f'/\eta \int_o^\eta f\eta\ d\eta = (\eta s)' \tag{2.15}$$

with boundary conditions

$$f(\eta) = 0 \qquad \text{as } \eta \text{ approaches infinity}$$

$$f'(\eta) = 0 \qquad \text{at } \eta = 0$$

$$2\pi \int_o^\infty f^2\ (\eta)\ \eta\ d\eta = 1 \tag{2.16}$$

The last equation is unity only if the fluctuating terms are ignored. These terms can account for up to 7% of the source momentum (Seif 1981).

2.3 In The Finite Environment

For the confined jet, the entrainment must be fed by the return flow. Outside the shear zone the flow is inviscid and governed by the Euler Equations from which it follows that

$$-\frac{1}{\rho}\frac{\partial}{\partial x}(P_\infty) = U_\infty \frac{\partial}{\partial x}(U_\infty) = \frac{\partial}{\partial x}\left(\frac{U_\infty^2}{2}\right)$$

Capp has shown that if it is assumed that the return flow is uniformly distributed across the total cross-sectional area, the momentum integral reduces to

$$\frac{\partial}{\partial x}\int_0^R \left((U^2 + \overline{u}^2 - \frac{\overline{u^2+w^2}}{2}) - \frac{U_\infty^2}{2}\right) 2\pi r dr = 0$$

or

$$M(x) = \int_0^{R_s} (U^2 + \overline{u}^2 - \frac{\overline{u^2+w^2}}{2})\, 2\pi r dr = M_o - \frac{U_\infty^2 A_r}{2} \qquad (2.17)$$

where

A_r = Room area

R_s = Separation point between the region of laminar back flow and zero of turbulent jet.

Thus the momentum in the jet is continuously reduced by the presence of the return flow as one proceeds away from the exit plane. Capp believed the problem in the experiments which preceeded him to be that the rooms were small enough that the momentum loss to the backflow was significant. As a result he alleged that the profiles measured did not represent a true jet in an infinite environment, but rather a jet in a closed room.

CHAPTER 3

DESCRIPTION OF THE ENVIRONMENT

3.1: Jet Facility

The jet itself was of one inch exit diameter and was the same as that used by Capp (1983). However, a much larger enclosure (described below) was used in the present work. Hot-wire measurements with the three-dimensional traversing system were carried out at axial distances of from 0 to 50 exit diameters.

The jet exit Reynolds number was 9.3×10^4 insuring that the asymptotic jet was fully turbulent. The Mach number was 0.167 so that compressibility effects were negligible. The jet had previously been shown to be momentum conserving and self-preserving by the laser Doppler anemometer measurements of Capp (1983). The physical dimensions of the jet are shown in Figure (3-1). The three-dimensional traversing system is shown in Figure (3-2). Driving the flow was a Dayton Model 4C108, 10 5/8 in. dia. wheel, 1 H.P., 3450/2850 R.P.M. high pressure, paddle type blower. The speed was varied during calibration by means of an inverter.

A vibration isolater was installed between the blower and the diffuser section of the jet to reduce blower induced vibration (see Figure (3-1) part 1). Part 2, shows a slot and plate, through which the air escapes from the slot to the room. The slot allows the room to act as a big tank and decreases the effect of the blower fluctuations on the exit flow.

Spatial inhomogeneities in the mean flow and swirl were removed by using wire screen and honey comb (plastic straws) upstream of the contraction. The first contraction of 16:1 was a matched cubic based on

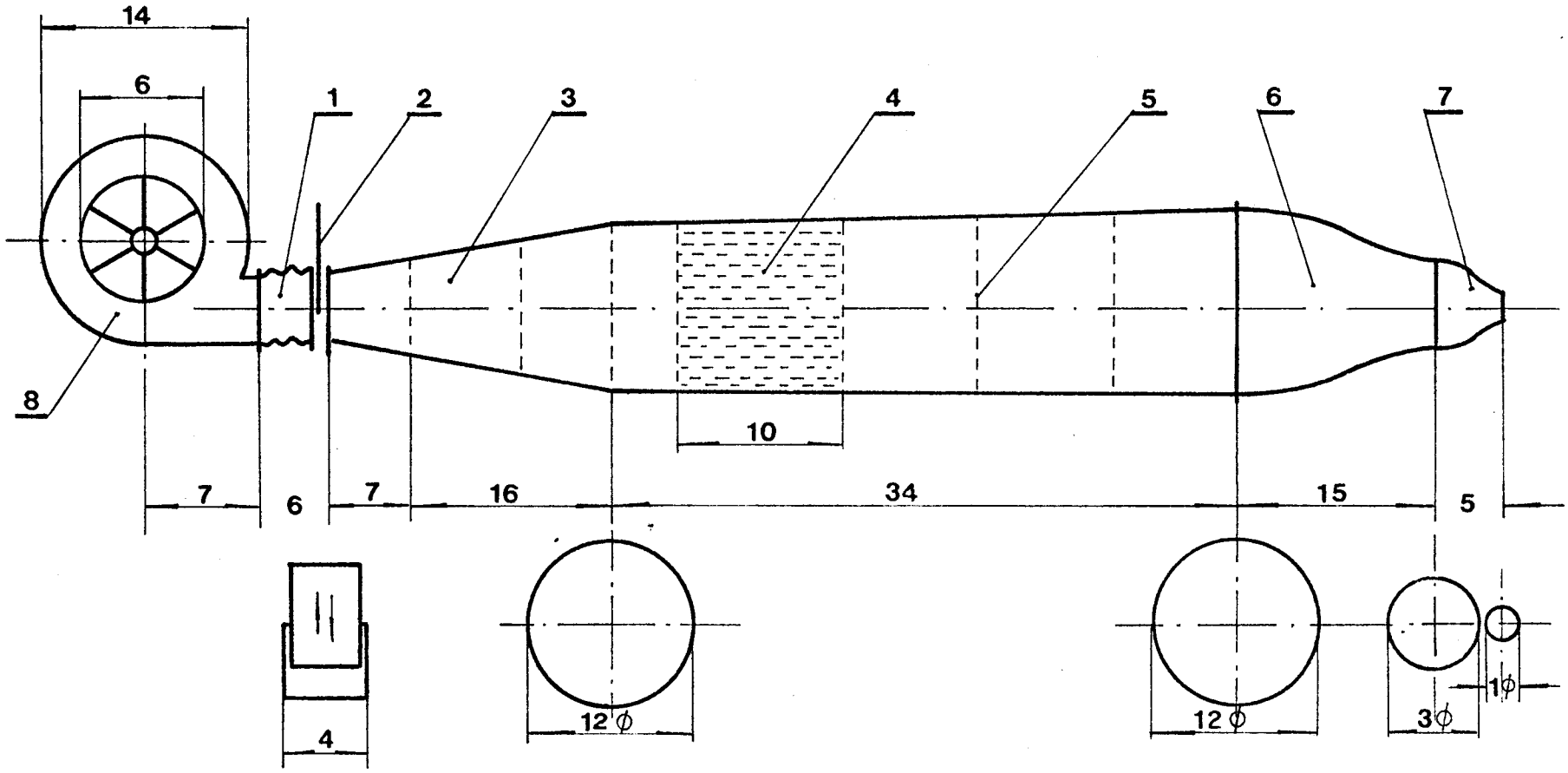

FIGURE: 3—1 JET FACILITY (ALL DIMENSIONS IN INCHES)

1. VIBRATION ISOLATION
2. SLOT AND PLATE
3. DIFFUSER
4. HONEY COMB
5. SCREEN
6. NOZZLE
7. JET
8. BLOWER

the work of Morel (1975). The second contraction was 9:1 was added to bring the exit to the required one inch diameter. The last contraction was constructed using a fifth order polynomial. As demonstrated by Tanatichat (1980), such a curvature produces a more uniform mean velocity distribution over a shorter length than do other alternatives.

Figures (3-2), (3-3), (3-4), (3-5), (3-6), (3-7) show measurements of the mean velocity which confirm that the mean velocity distribution remained symmetrical as it developed downstream.. The exit profile is shown in Figure (3-8).

Figure (3-9) shows the confined jet. In our experiment x=8.5, -x=6.7, y=7.5, -y=7.5, z=34.6, -z=16 (all dimension in feet). The enclosure measurements are indicated in Figure (3-10).

Centerline velocity measurements were taken from x/D of 0 to 50. In the non-dimensional radial direction, r/x, these measurements spanned from -15 inches to 15 inches.

3.2 Traversing System, Instrumentation and Signal Processing

The traversing system is shown in Figure (3-11). The three-dimensional traversing system is under the minicomputer and microcomputer control. A data file is created containing the positions (x,y,z) of interest, then the data are taken automatically at the points contained in the file.

The limits of the traversing system as placed for this experiment are from the exit plane to x=46, y=46, z=55 inches. The maximum axial position corresponds to 55 diameters. The positioning accuracy is estimated as better than 0.002 inches.

Figure (3-12) shows the signal processing equipment. The hot-wire is mounted on the three-dimensional traversing system. The signal from

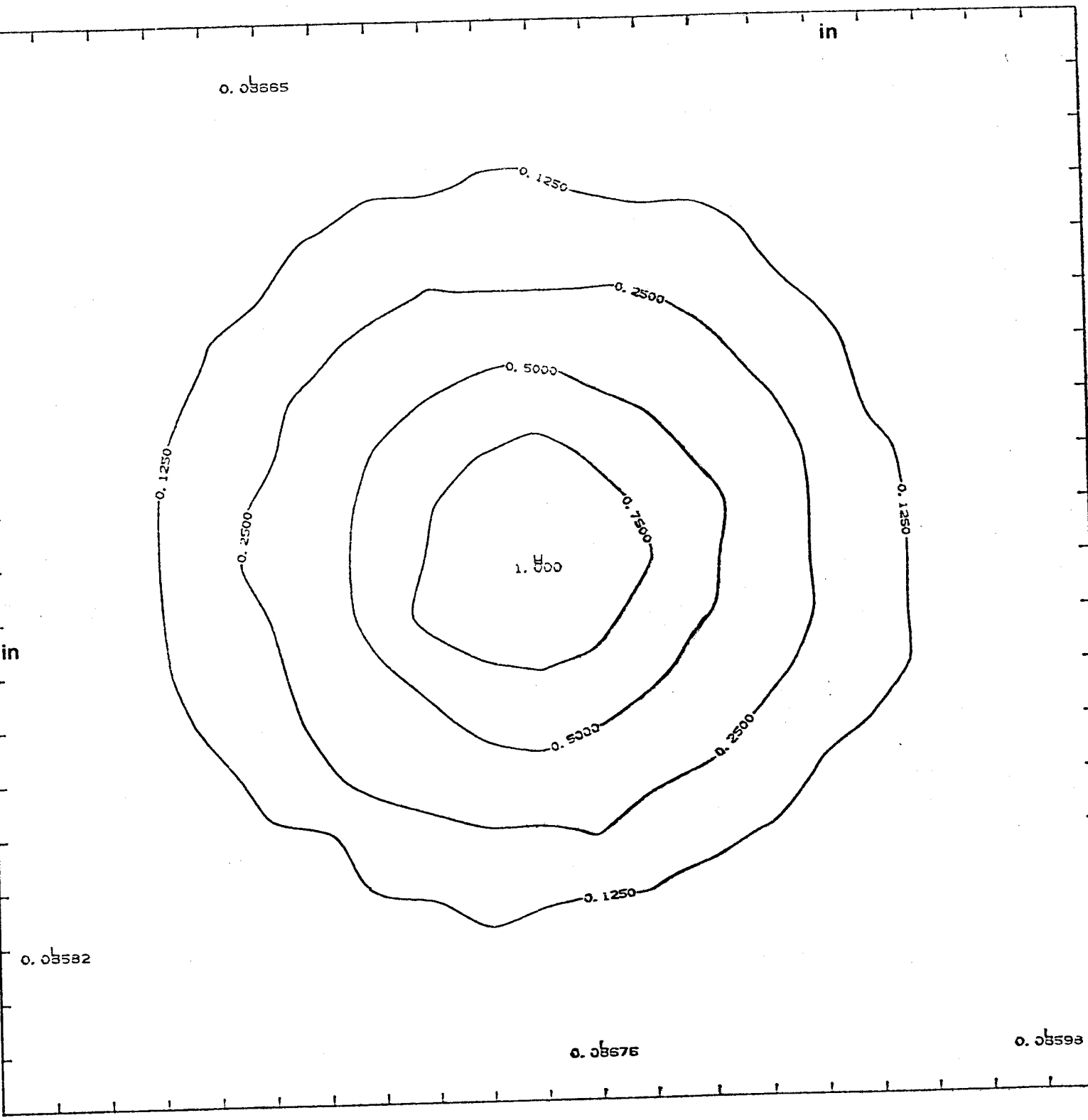

Figure 3-2 Hot-Wire Measurements u/u_c Constant Velocity Contours x/D = 30

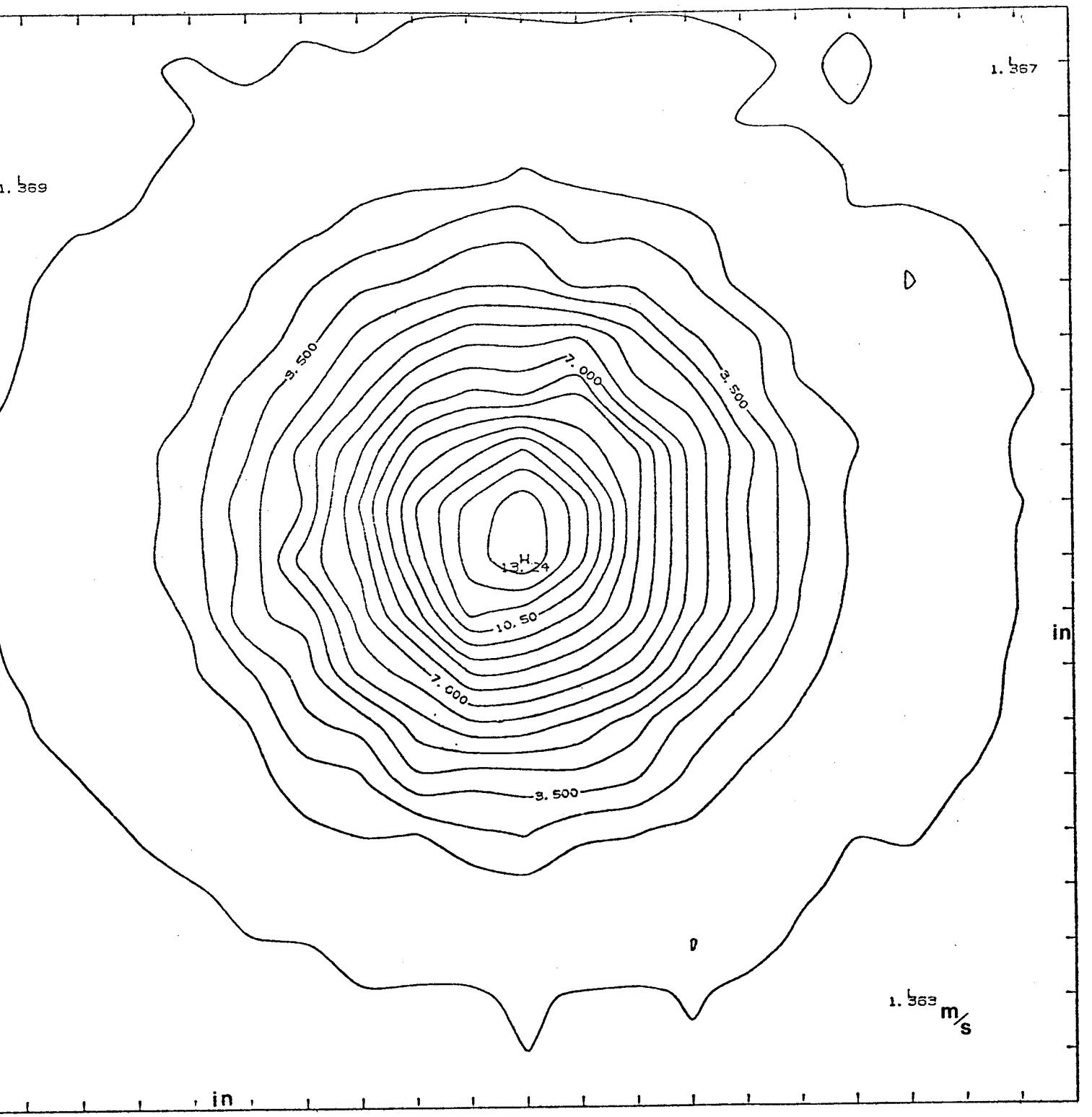

Figure 3-3 Hot-Wire Measurements Constant Velocity Contours x/D = 30

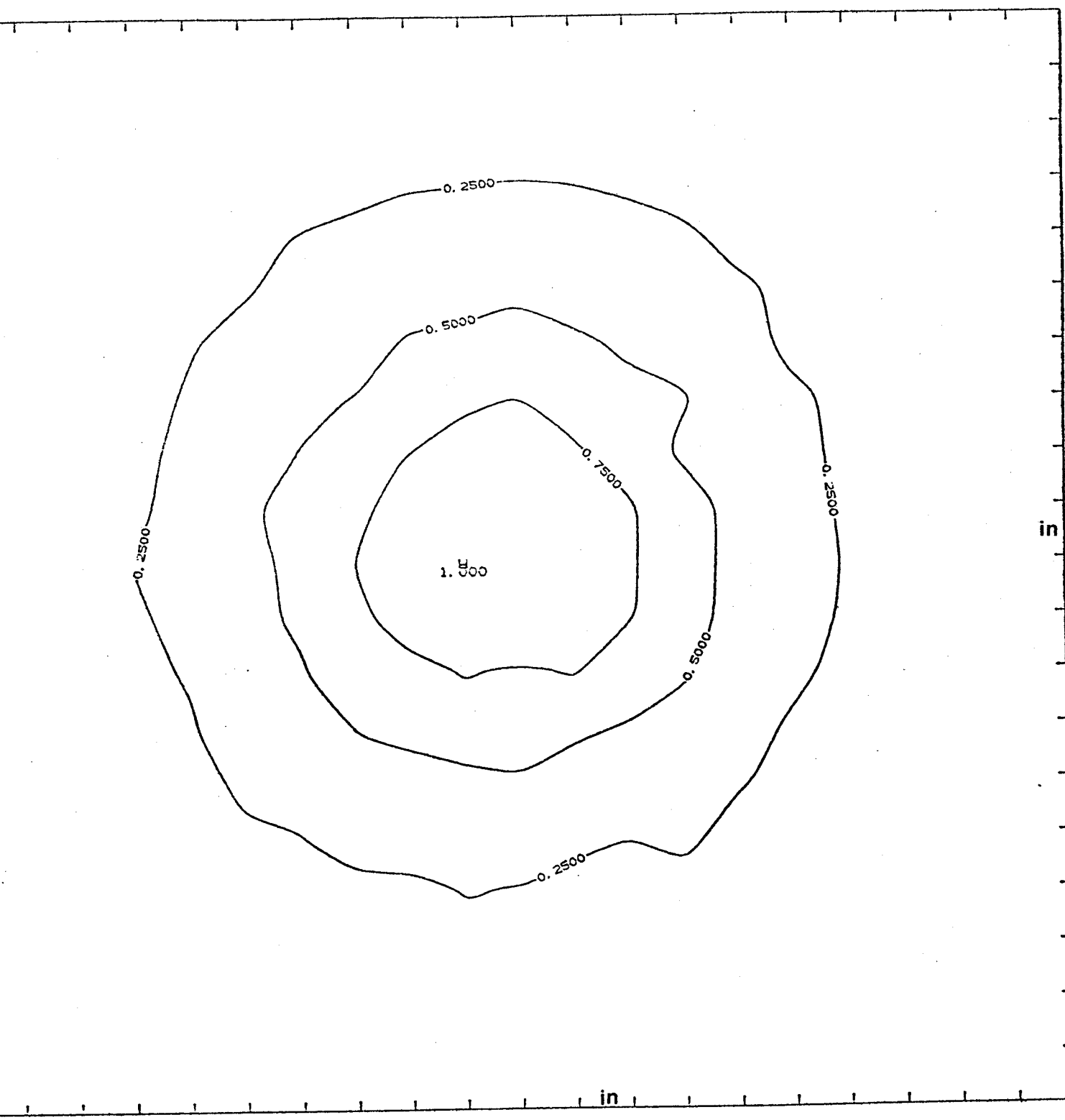

Figure 3-4 Hot-Wire Measurements u/u_c Constant Velocity Contours x/D = 40

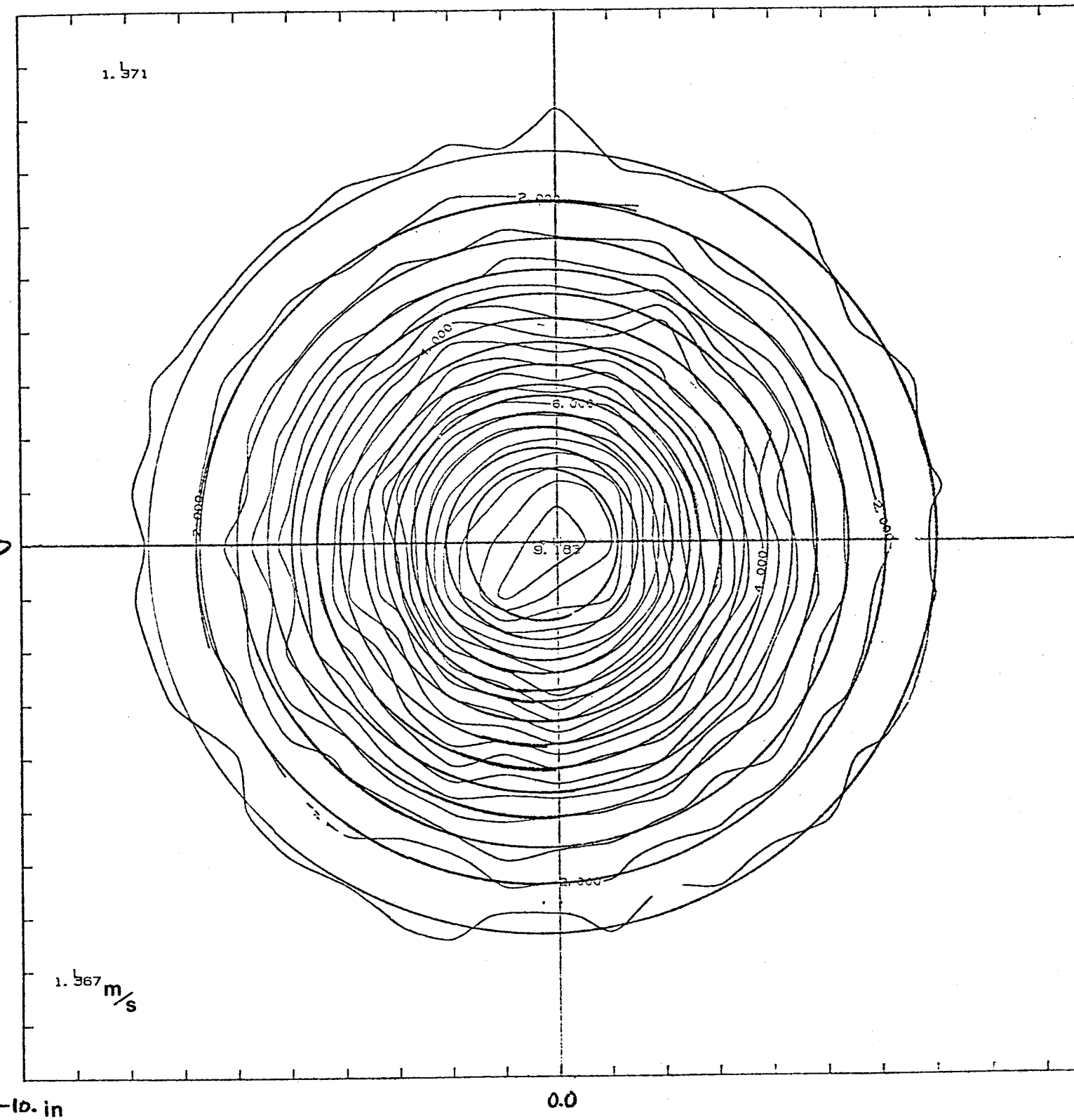

Figure 3-5 Hot-Wire Measurements Constant Velocity Contours x/D = 40

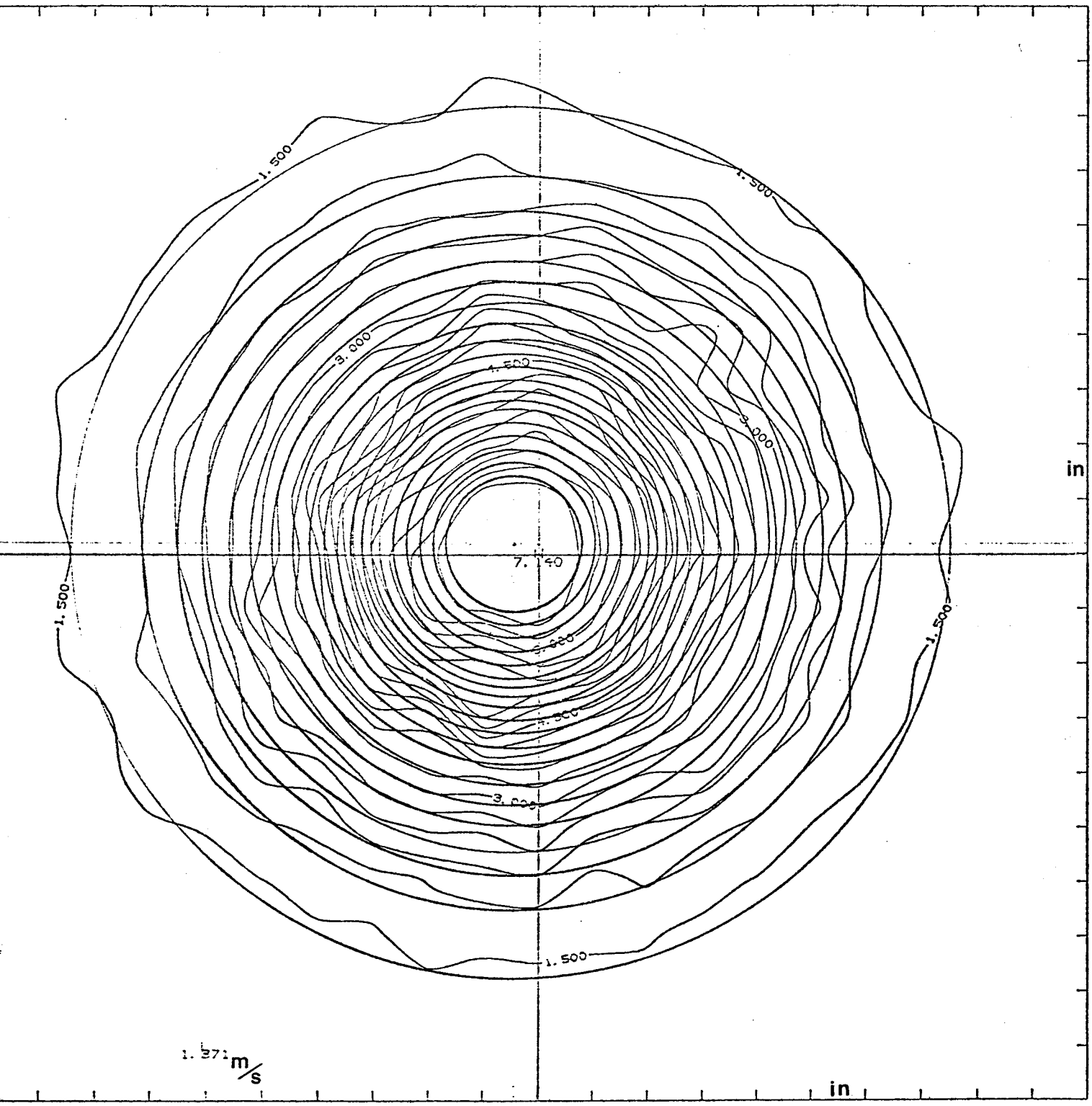

Figure 3-6 Hot-Wire Measurements Constant Velocity Contours x/d = 50

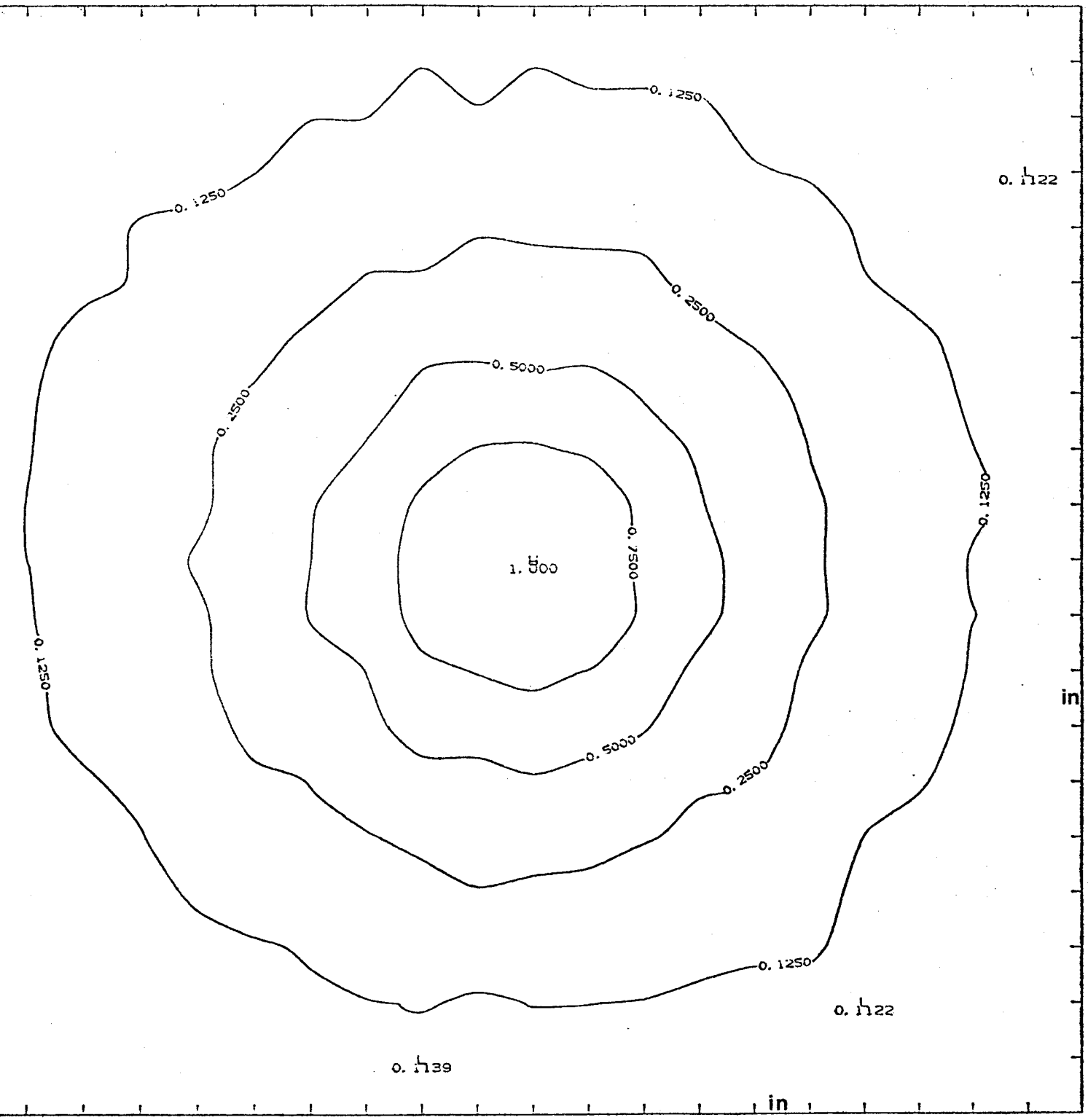

Figure 3-7 Hot-Wire Measurements u/u_c Constant Velocity Contours x/D = 50

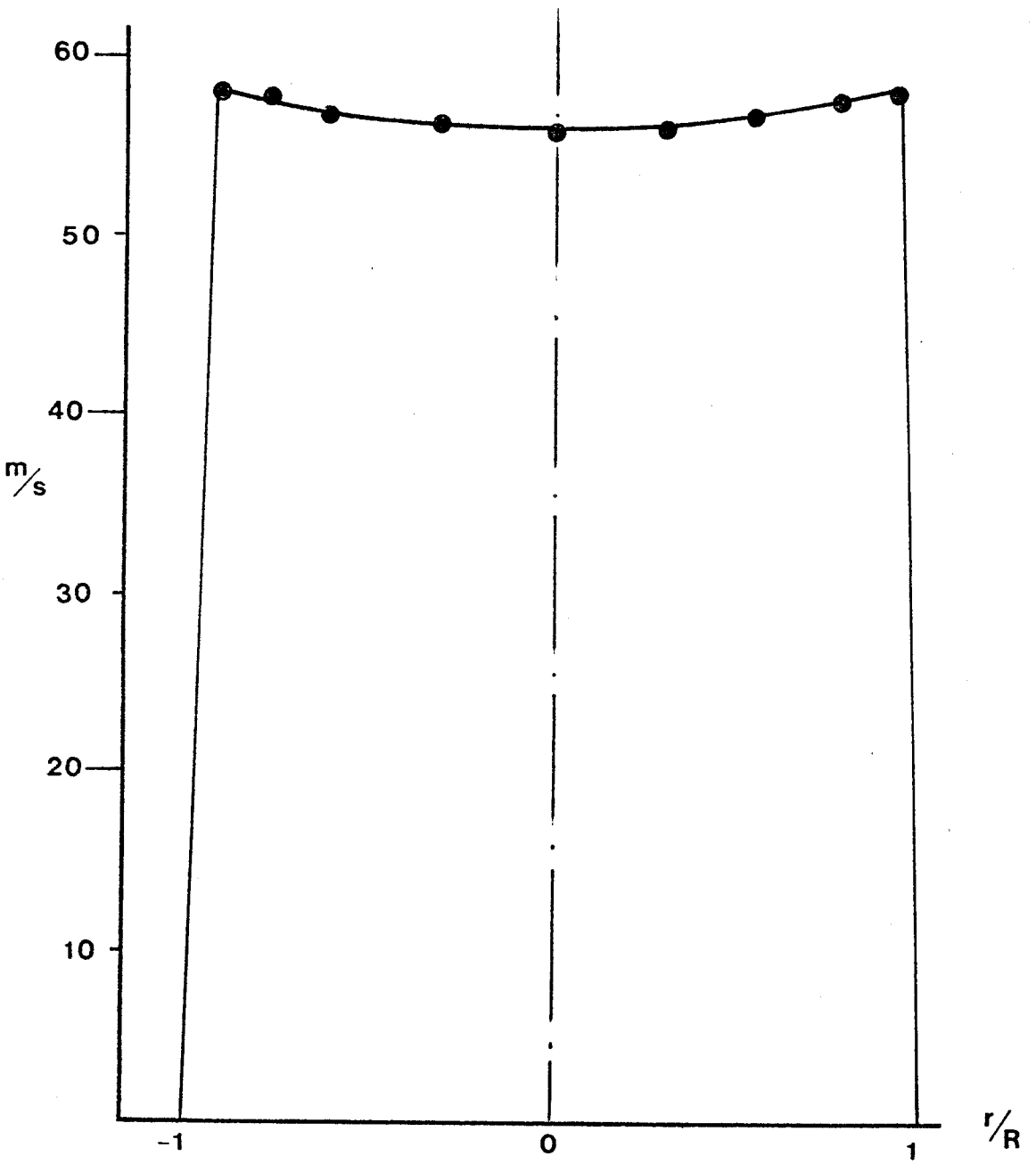

FIG. 3-8 JET EXIT PROFILE

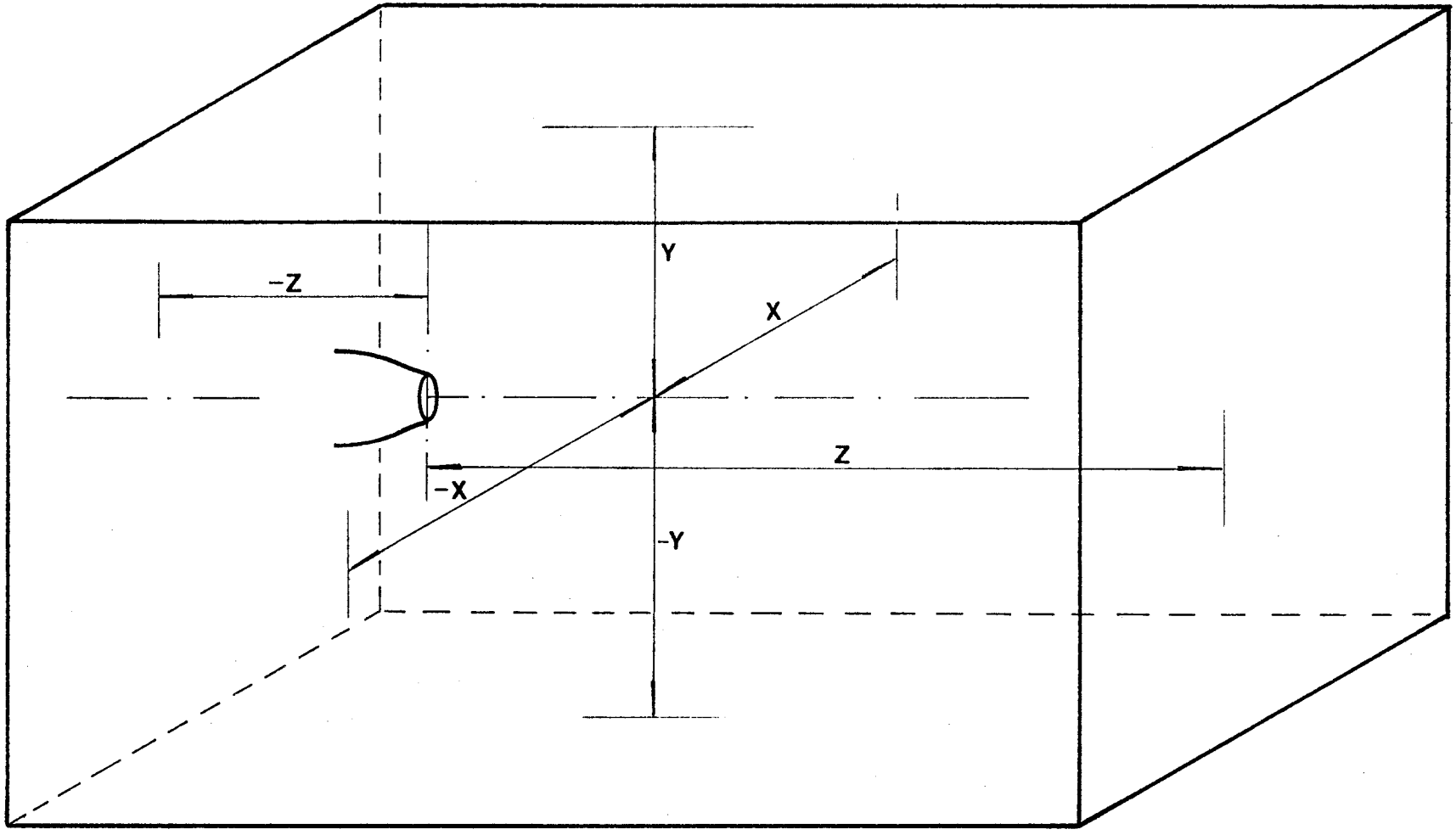

FIGURE: 3—9 A CONFINED JET

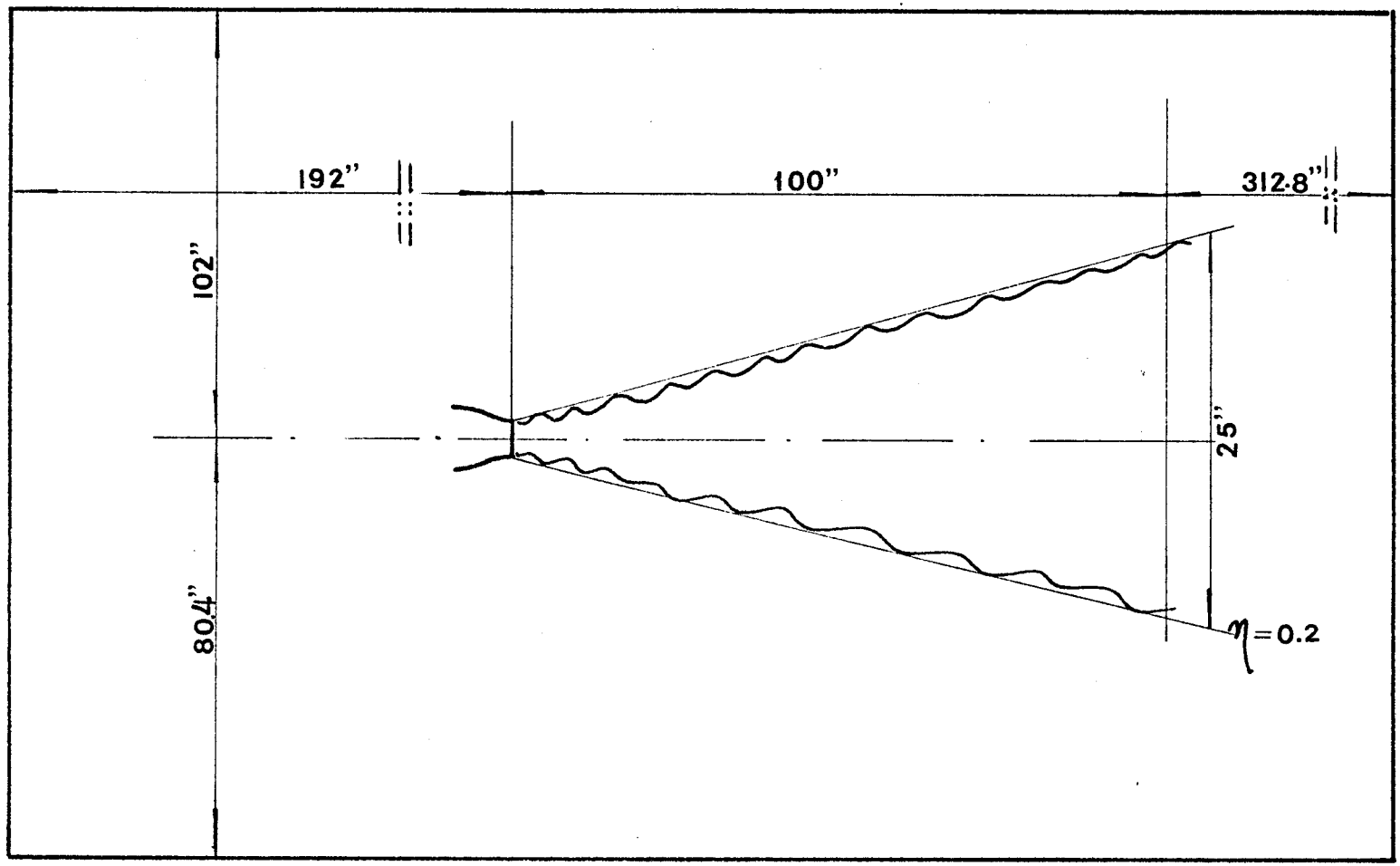

FIGURE 3—10 THE ENCLOSURE MEASUREMENT

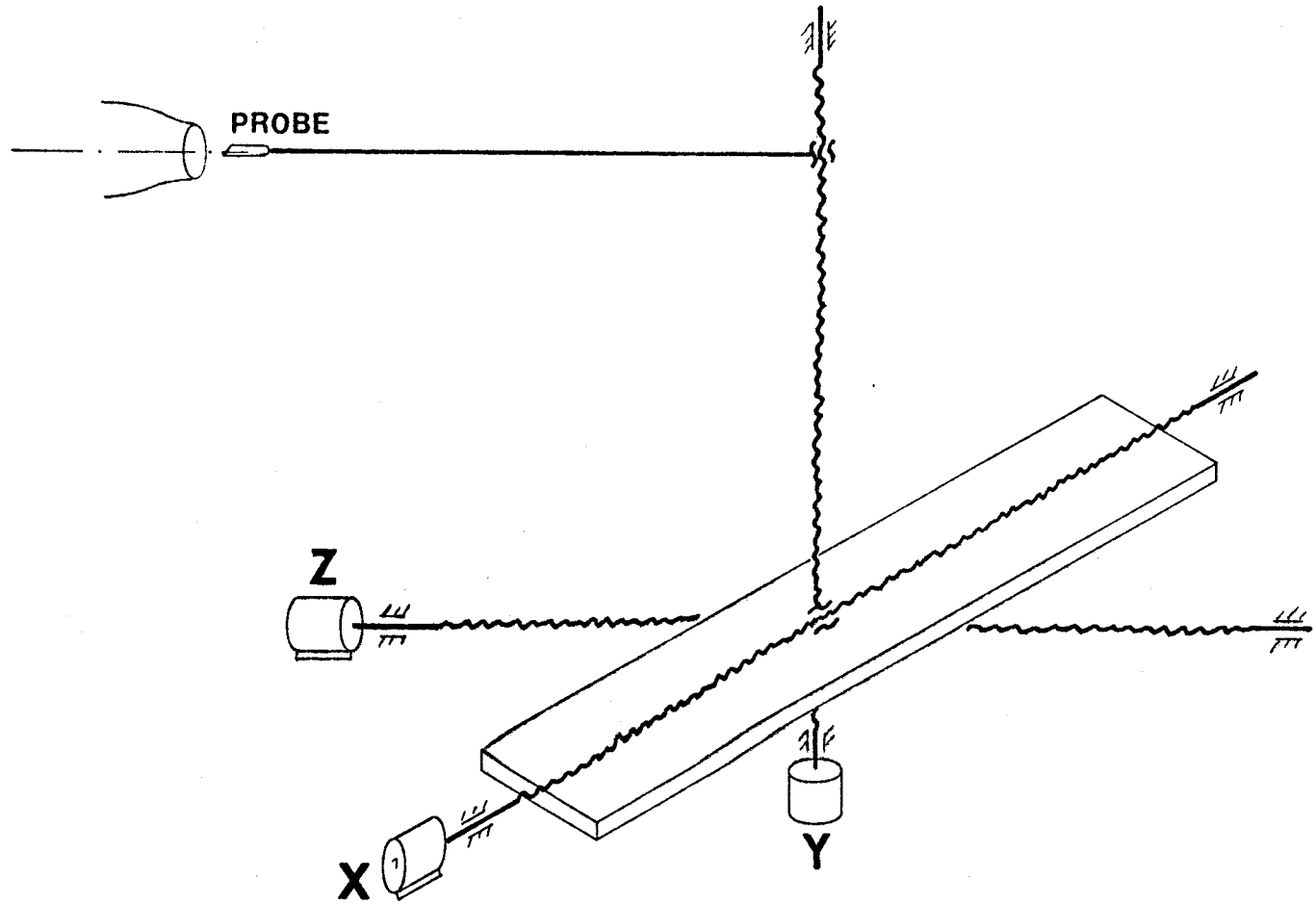

FIGURE: 3–11 TRAVERSING SYSTEM

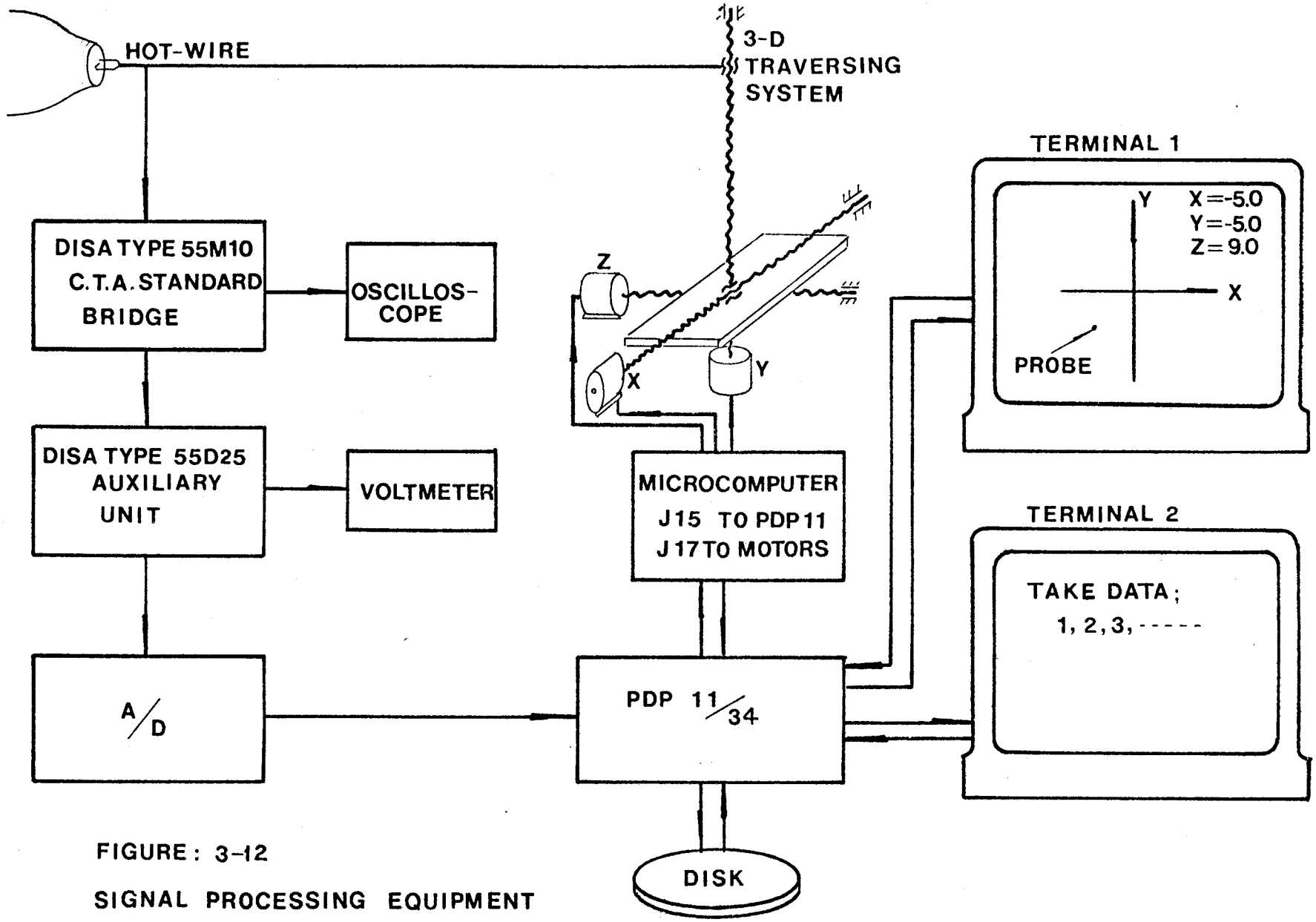

FIGURE: 3-12

SIGNAL PROCESSING EQUIPMENT

the hot-wire anemometer constant temperature standard bridge (DISA type 55M10), is connected to the oscilloscope and an auxillary unit (Disa type 55M25). The oscilloscope is for observation, and the auxillary unit is for changing the D.C. offset of the output voltage. A Phoenix A/D converter changes the output signal from analog to digital. A PDP 11/34 minicomputer was used both to store and process the data.

Two terminals were used. One of them was used to display the coordinates of the traversing system, which indicated the position of probe (x,y,z), while another one showed the number of blocks of data taken.

3.3: Analysis of Hot-wire Cross Flow Error

Figure (3-13) shows the measured rms axial velocity fluctuations normalized to the local mean velocity. In the jet the minimum turbulence intensity is at the centerline and is about 25%. As the radial coordinate increases, u'/U increases rapidly. As turbulence intensity increases, the hot-wire measurement error also increases.

The hot-wire cannot distinguish the flow direction since the flow from any direction can carry heat from the hot-wire. Thus for both positive and negative velocities the hot-wire response is the same. This phenomenon leads to the so-called rectification errors, (Tutu and Chevray 1975) which are important only at the outer edge of the flow for single wire probes.

A more serious limitation for this experiment is the so-called cross-flow error. If w is the component of the flow normal to the wire and the mean velocity is assumed to be in the x-direction, the effective cooling velocity for the wire is

$$u_m^2 = (U + u)^2 + w^2 \qquad (3.1)$$

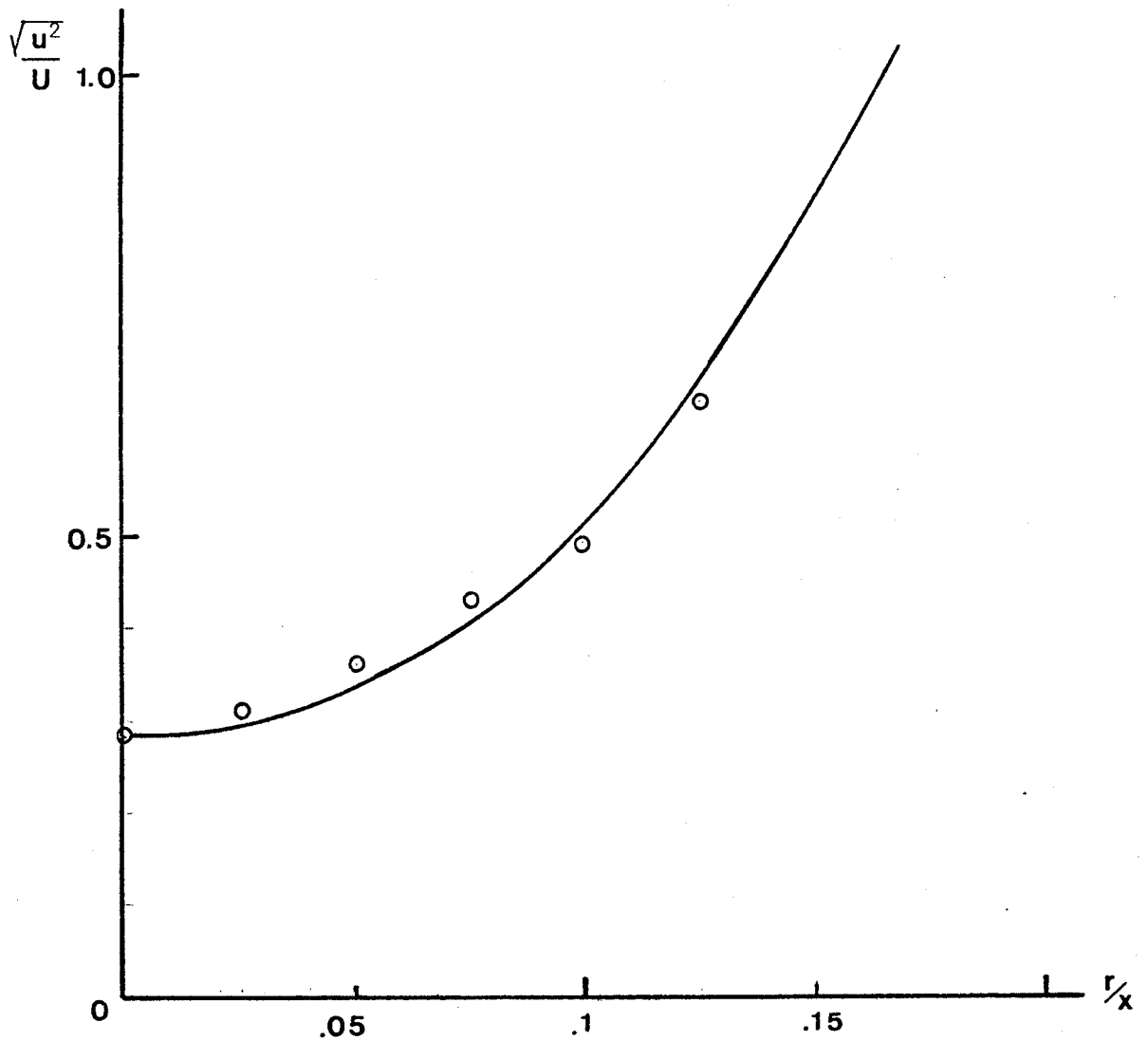

Figure 3-13 Measured RMS Axial Velocity Fluctuation Normalized to the Local Mean Velocity (Capp 1983)

By assuming the fluctuating terms to be small relative to the mean, the right hand side of equation (3.1) can be expanded in a binomial expansion to yield an expression for the average of the measured velocity given by

$$U_m \cong U \{1 + \frac{1}{2} \frac{\overline{w^2}}{U^2} + h.t.\} \qquad (3.2)$$

The higher terms become significant quickly as the turbulence level is increased.

Figure 3-14 illustrates the effect of the cross-flow error on the jet profile using Capp's LDA measurements of the U, $\overline{w^2}$. These will be compared later to the profiles measured with a hot-wire in this experiment.

Hot-wires are minimally contaminated by high intensity turbulence effects only to turbulence intensities of 20-30% (v. Hinze 1975), which is about the intensity of the jet centerline. When r/x=0.1 the local turbulence intensity is already 50% and the velocity measurement errors are significant. By r/x=0.2 the local turbulence intensity is 100% and the hot-wire measurements are seriously in error.

An overall consequence of these effects is that a properly calibrated wire must always measure too high in a turbulent flow. Thus mean profiles measured in a jet should be higher than those measured by the laser Doppler anemometer which does not suffer from the rectification and cross-flow errors.

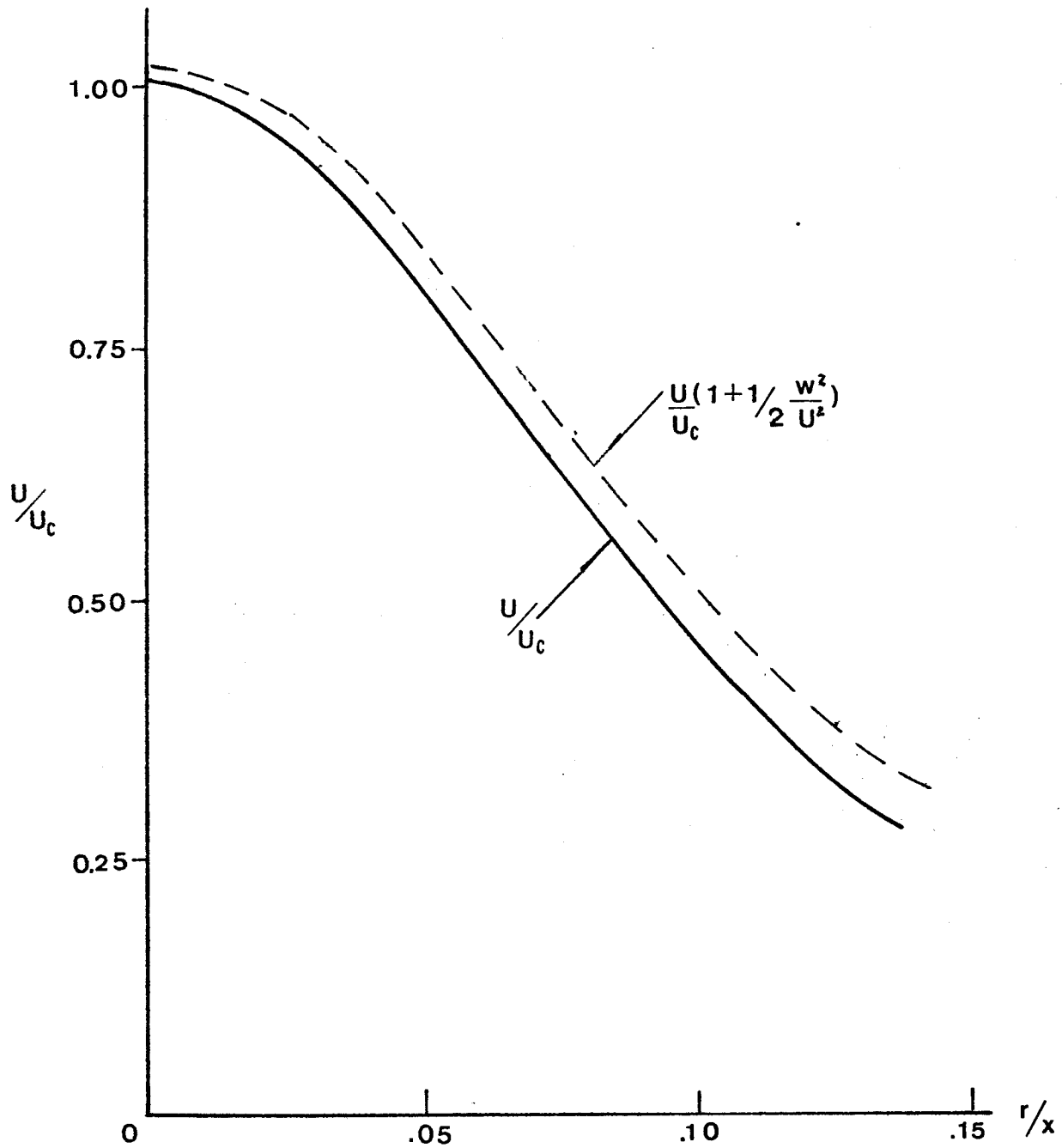

FIG. 3—14 CROSS-FLOW ERROR(FROM CAPP'S DATA)

3.4 Measurement Techniques

Turbulent flow measurement almost always involves random signal processing. In this experiment it is necessary to obtain the time-averaged velocity defined by

$$U_T = 1/T \int_0^T u(t)\, dt \tag{3.3}$$

When the T approaches infinity, the U_T will approach the true average. Estimates based on finite times, however, will suffer from statistical error.

If the process is Ergodic, the random variable must become uncorrelated, with itself and an integral scale T_u exists. Figure (3-15) shows T_u defined by

$$T_u = \int_0^\infty \rho_u\ (\tau)\ d\tau \tag{3.4}$$

From George (1979) the relative error, the fluctuation level of the signal itself, and the integral scale are related as follows:

$$\varepsilon^2 = 2T_u/T\ [\sigma_u/U]^2 \tag{3.5}$$

where

T = averaging time

T_u = integral scale

If samples are taken at only discrete times at time spacings greater than two integral scales the relative error reduces to

$$\varepsilon^2 = (1/N)(\sigma_u/N)^2 \tag{3.6}$$

where N is the number of samples.

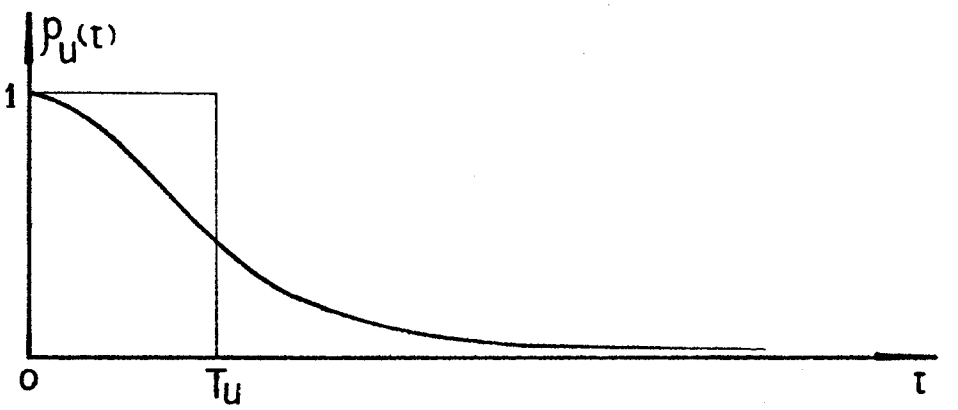

a. INTEGRAL SCALE

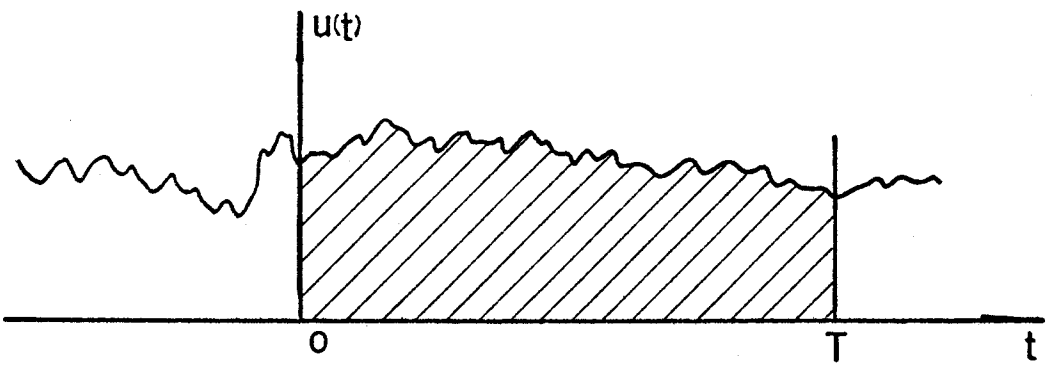

b. TIME AVERAGE

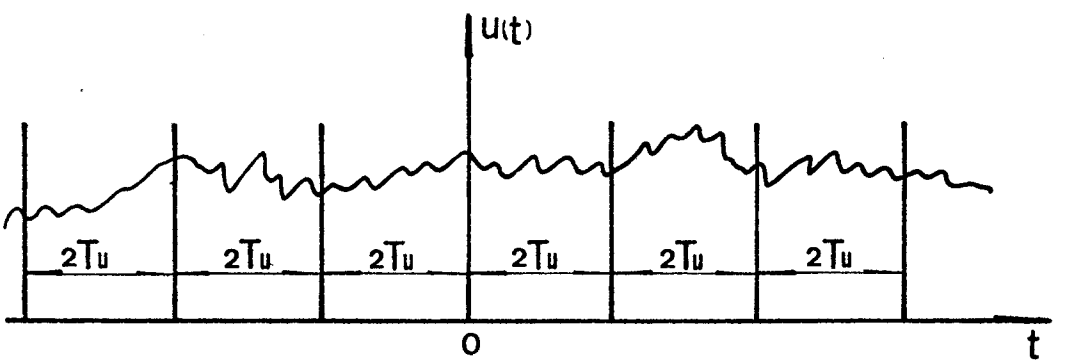

C. STATISTICALLY INDEPENDENT

FIGURE: 3—15 ILLUSTRATION OF AVERAGING CRITERION

In this experiment every data point represents an average over 1024 independent samples. In addition, the velocity grid at each downstream location consists of more than 400 points. The statistical error can be estimated from equation (3.6) above as

$$\varepsilon^2 = \frac{1}{1024} (\sigma_u/\bar{u})^2 \tag{3.7}$$

This corresponds to about 0.8% at the centerline and 1.5% at the half velocity point.

CHAPTER 4

THE RESULTS

4.1 Centerline Velocity Values

Figure (4-1) shows centerline velocity measurement from the jet exit x' = 0 to x' = 40 in. Recall that the mean velocity was the average of 1024 data points..

The data can be plotted as U_o/U_C, which when self-similarity is achieved should be linear in x/D. Figure (4-2) shows the centerline decay rate plotted in this manner. Even though only data to x/D = 40 are used, the resulting plot is quickly asymptotic to a straight line. The straight line of equation (2.13) for the jet centerline decay rate is given by

$$U_o/U_o = 1/B_u\ (x'/D - X_o/D)$$

U_o = Jet exit velocity

U_c = Centerline velocity

x' = axial coordinate with respect to jet exit

x = axial coordinate with respect to virtual origin

x_o = x' - x

B_u = Empirical constant

The centerline velocity decay, constants for the present experiment were

Hot-wire measurement $B_u = 5.87,\ x_o = 3.26$

Pitot tube measurements $B_u = 5.9,\ x_o = 0.64$

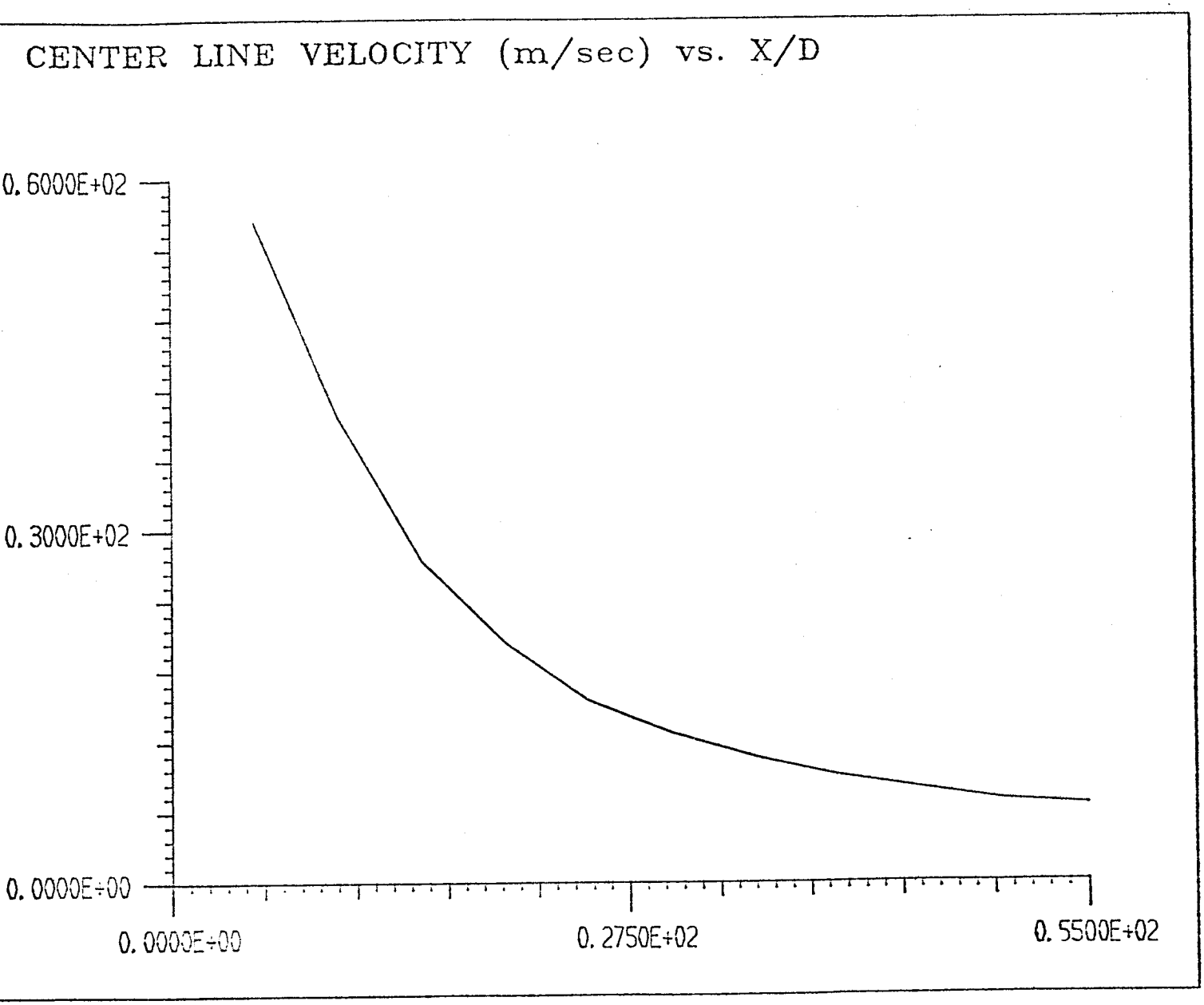

Figure 4-1 Hot-Wire Measurements of Centerline Velocity

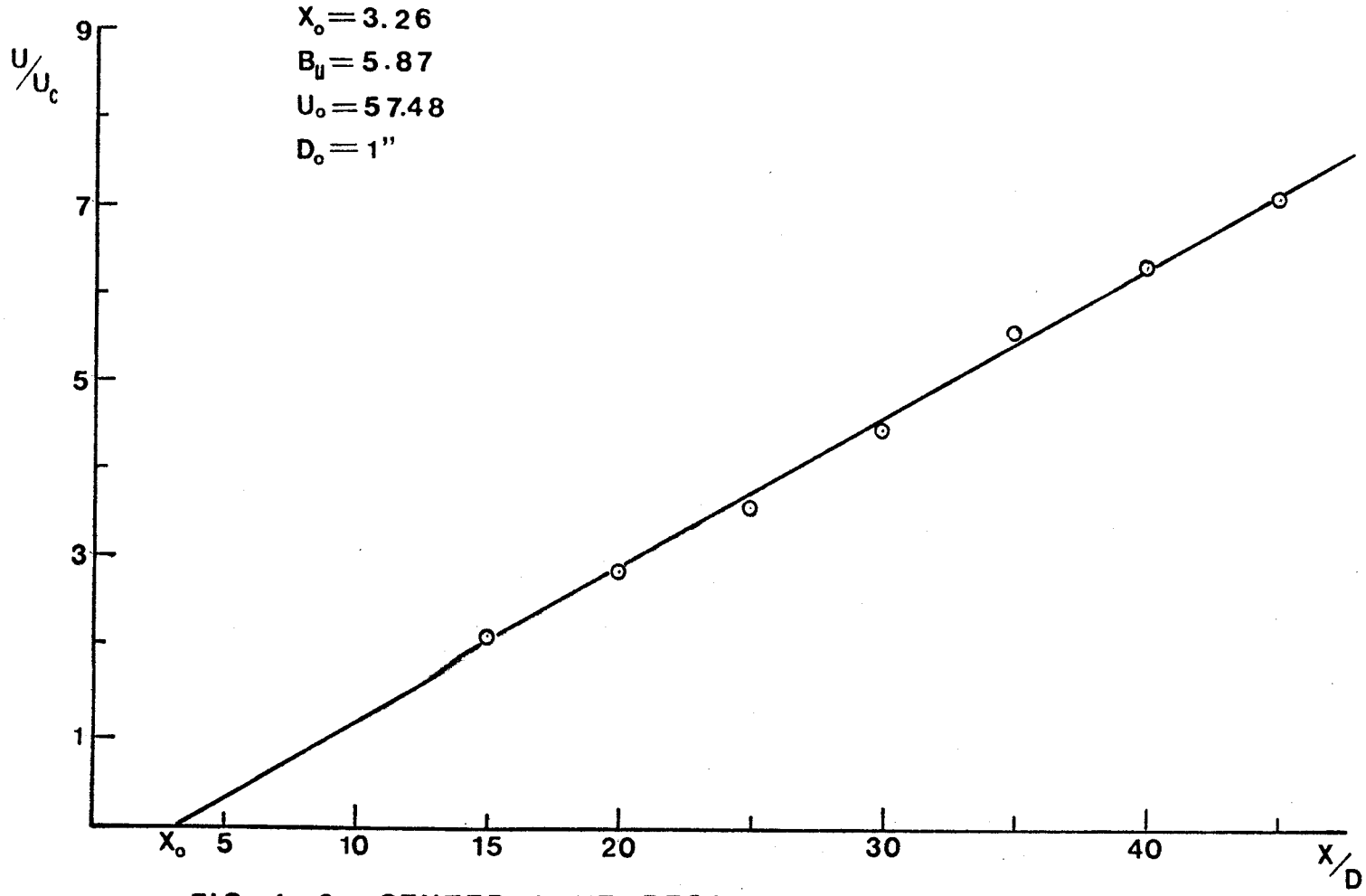

FIG. 4—2 CENTER—LINE DECAY RATE

These can be compared with the results of other authors.

1. Wygnanski and Fiedler (1969): $B_u = 5.9$ (The authors of this paper did not document a value for the decay rate, so their value of B_u has been approximated from a straight line as drawn on their plot for centerline values using only data for $x/D < 50$. A substantially lower value is obtained if data beyond this point are used.
2. Hinze and van der Hegge Zignen (1949) $B_u = 5.9$ (hot-wires, $x/D < 50$)
3. Seif (1981) $B_u = 5.8$ (calculated from Reynolds stress model)
4. Rodi (1975) $B_u = 6.0$ (hot-wires, $x/D < 80$)
5. Capp (1983) $B_u = 5.8$ (LDA, $x/D \leq 100$)

If Capp's centerline values are used to calculate what a hot-wire would measure given the cross-flow error a value of $B_u = 5.95$ is obtained, quite close to that obtained in this and the other hot-wire experiments.

4.2 The Mean Velocity Profile

Figure (4-3) shows the measured mean velocity profiles. Figure 4-4 plots U/U_c, the mean velocity normalized by the centerline velocity, versus $n = r/x-x_o$ where x_o was determined above as 3.26. The data from $x/D = 30$ to 50 show excellent collapse. Figure (4-5), shows the mean velocity profile data of the present investigation, compared with that of Seif (1981), and Capp (1983) and Wygnanski and Fiedler (1969). As expected, the hot-wire profiles are somewhat wider than the LDA profiles because of the cross-flow errors. Figure 4-6 shows a comparison between our measured hot-wire profile and that calculated earlier using Capp's data and the cross-flow error analysis given in Section 3.3. The

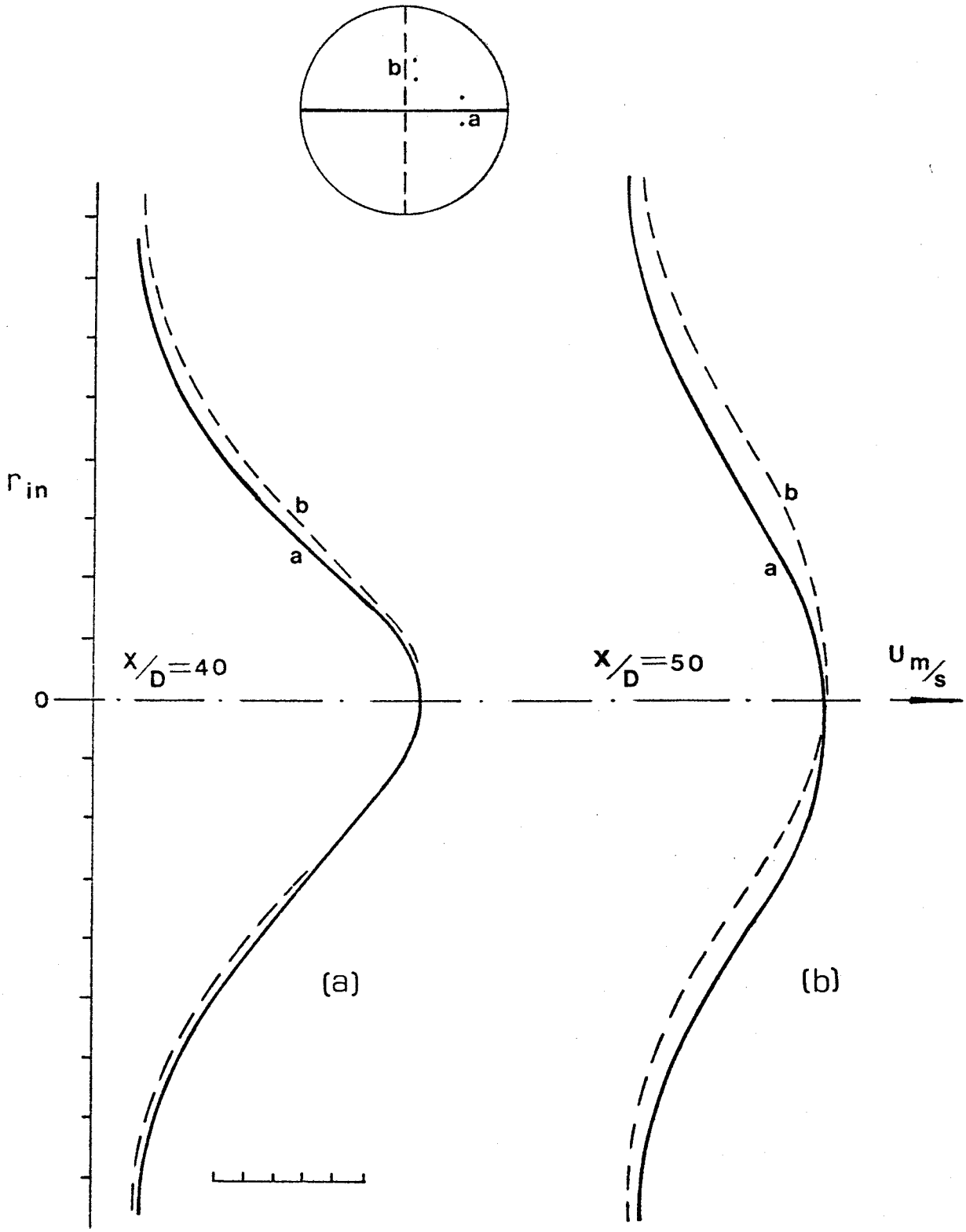

Figure 4-3 Measured Profiles of Mean Velocity (1)

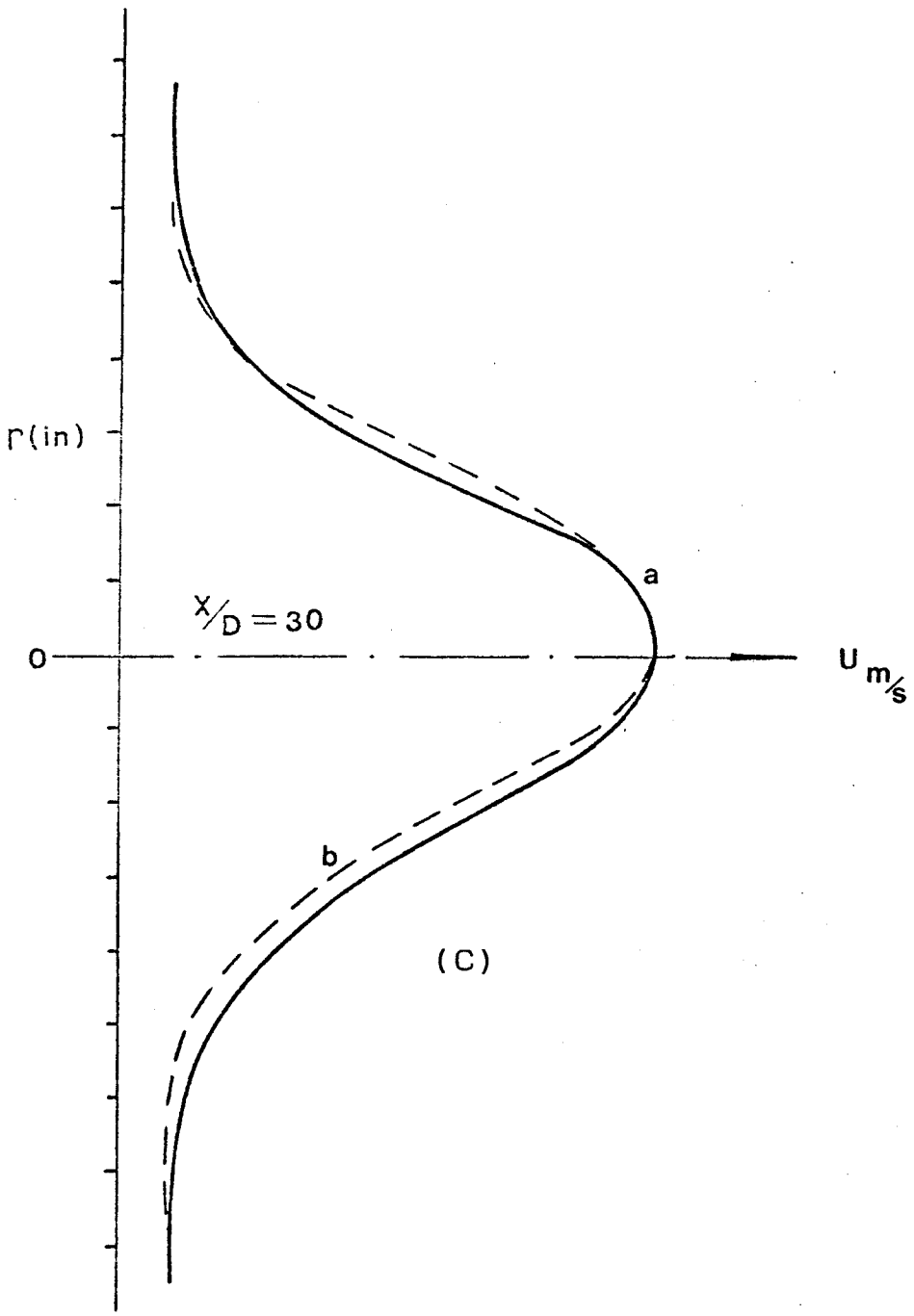

Figure 4-3 Measured Profiles of Mean Velocity (2)

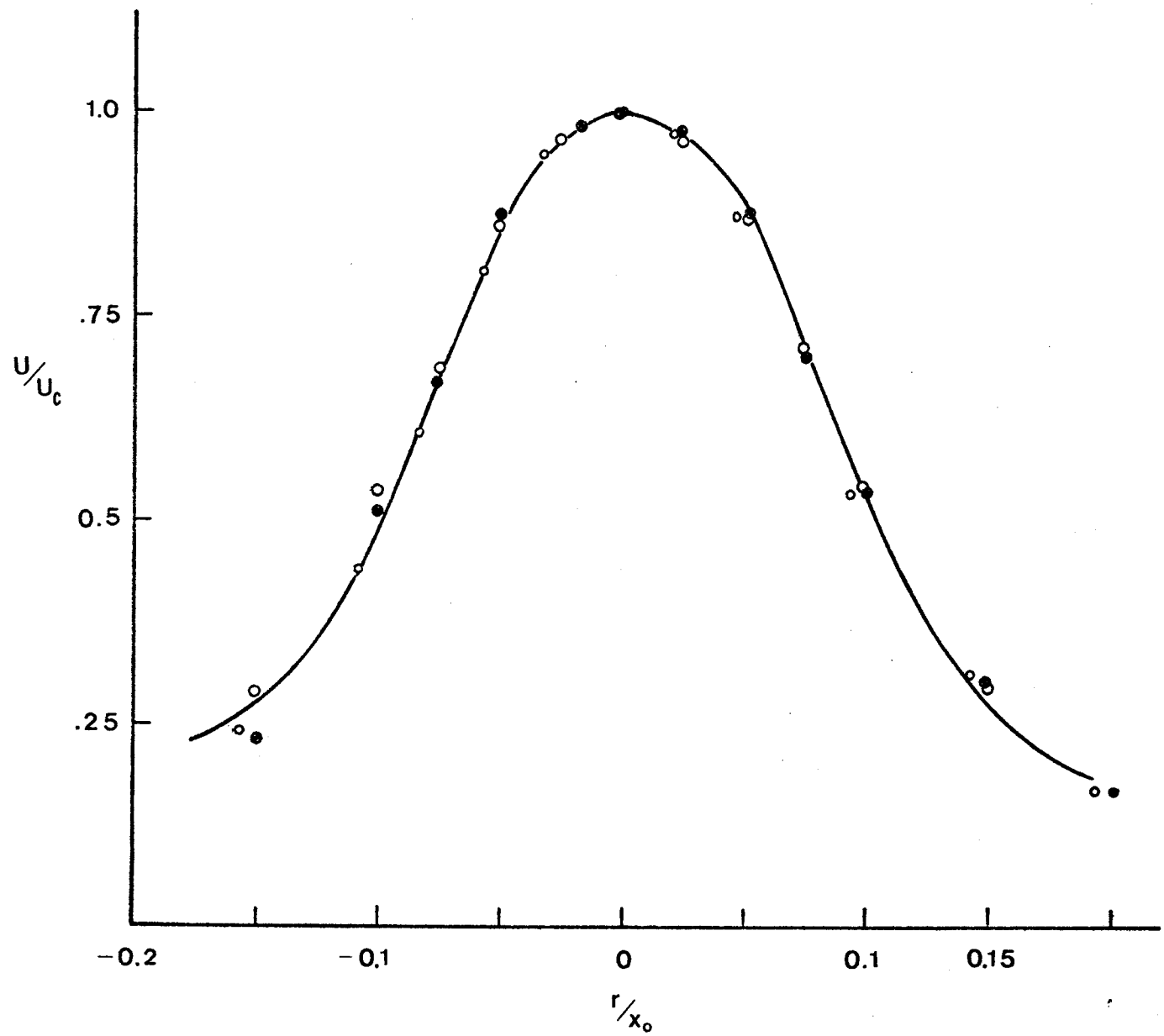

FIG. 4-4 NORMALIZED MEAN VELOCITY PROFILE

$X/D = 30$ —•, 40 —∘, 50 —∘,

$X_o = 3.26$

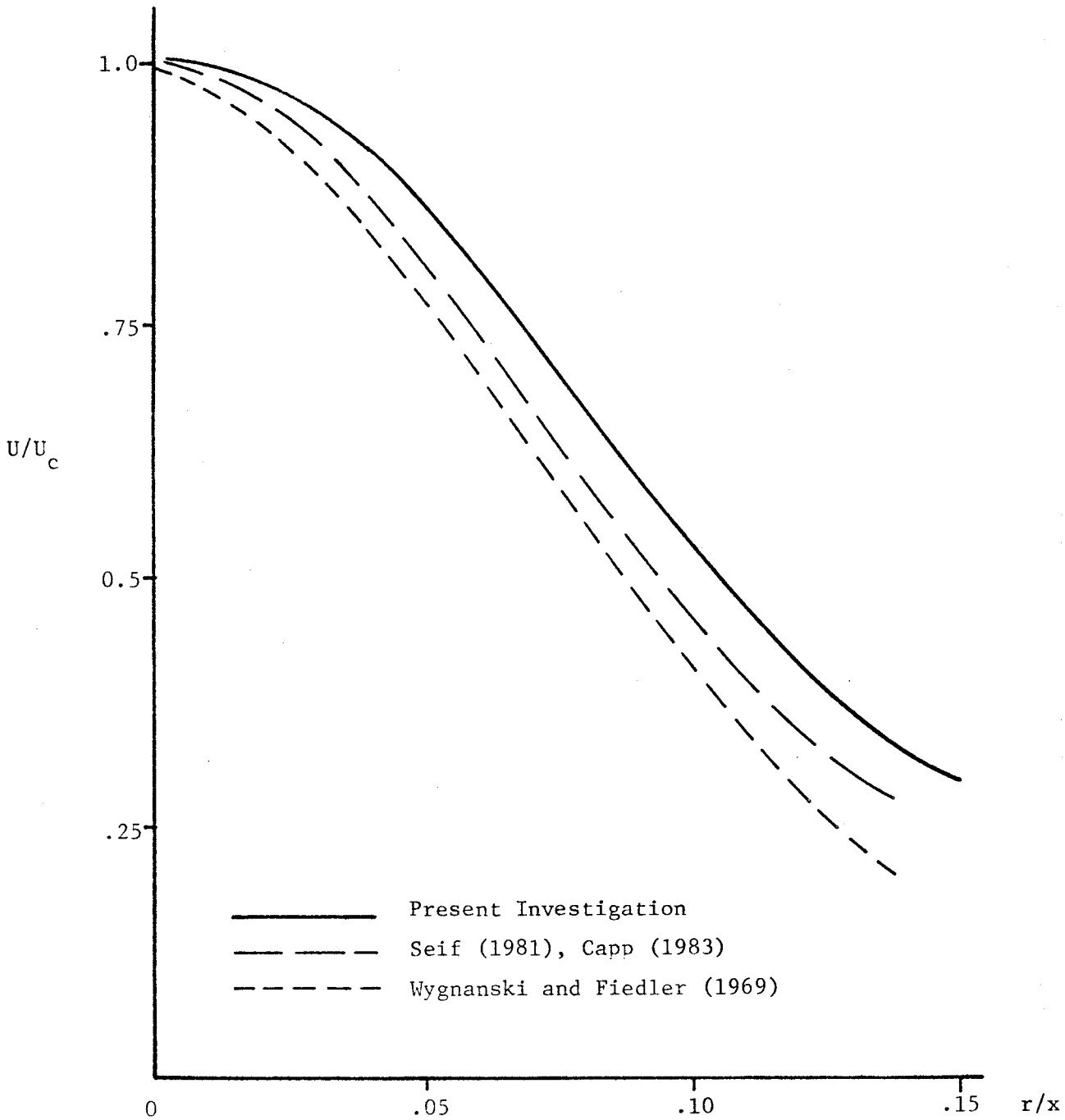

Figure 4-5 Mean Velocity Profile Compared to Others

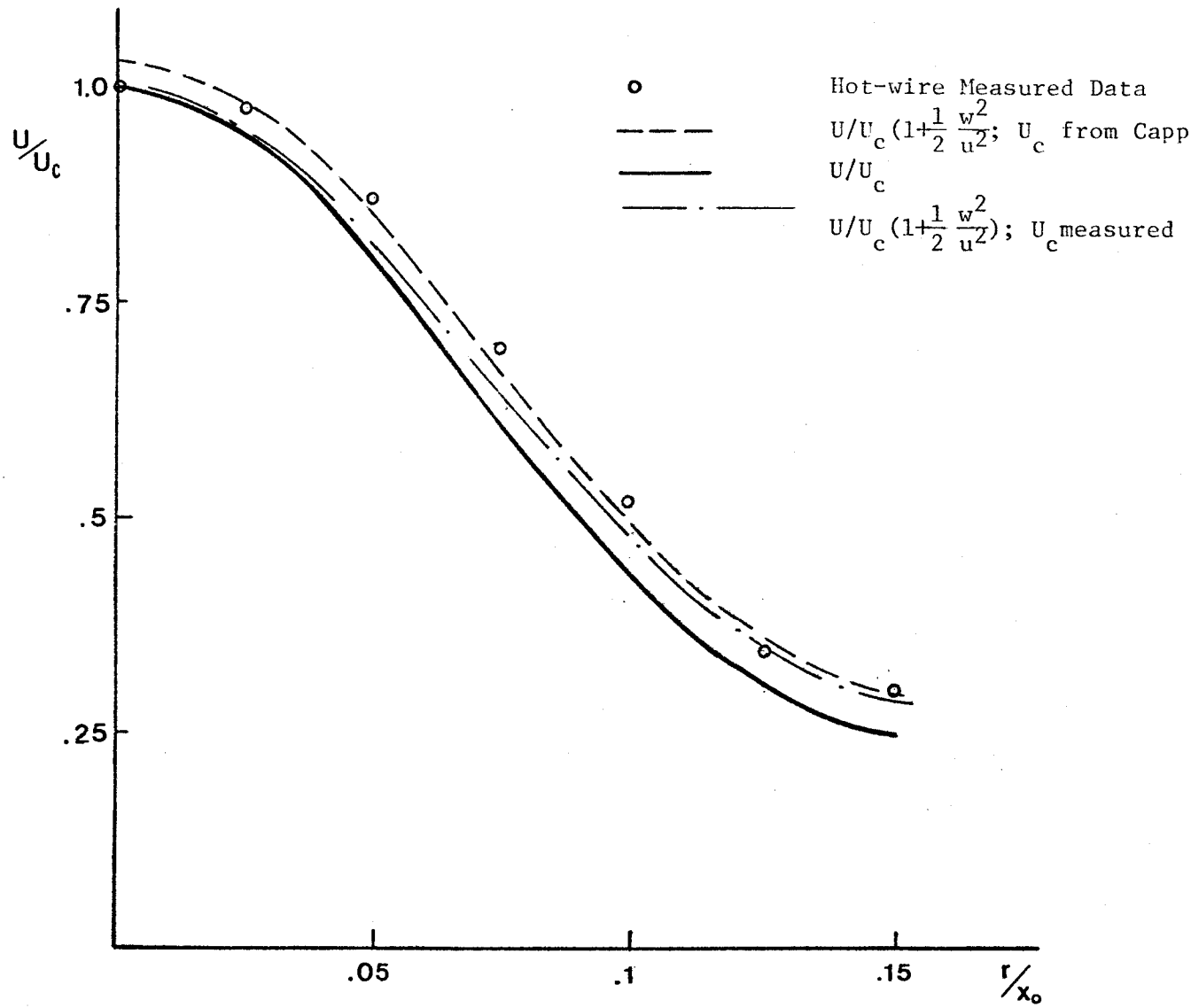

Figure 4-6 Comparison of Measured Mean Profile with Cross-Flow Error Estimate

agreement is quite gratifying especially in view of the fact that only data to x/D = 50 are used.

Capp presented one critical question in his dissertation: It is expected that mean values computed using LDA techniques are in general lower than CTA methods (see Buchhave, 1979). Since the center line velocity values display this pattern, why then is the LDA profile wider than those taken using CTA measurements? Clearly such is not the case and Capp's allegation that there must have been a more fundamental problem with the earlier experiments appears to be correct.

We can answer this question right now. Our measurements show CTA methods to produce results higher than LDA methods, as might be expected from the cross-flow analysis of the wire. The narrower profiles of the other investigators must be due to the modification of their flows by the return flow in their facilities and/or the boundary condition they placed on their experiments at large radius.

4.3 Concluding Statements on the Experimental Results

Capp used the LDA to measure the axisymmetric jet at x/D's of 70 and 100 and showed them to satisfy the momentum constraint. Although both Rodi and Wygnanski and Fiedler have measured jet half-widths of $\eta_{1/2} = 0.86$, the results of Capp's experimental program suggest a value closer to 0.095. Our experiments, when corrected for the cross-flow errors, are consistent with Capp's value of 0.095 and with his centerline decay rate of $B_u = 5.8$.

Capp said, "It is not yet clearly understood why the CTA techniques should produce a narrower velocity profile since previous experience would suggest the opposite." The results of this current experimental program strongly support Capp's allegation that the CTA

techniques should produce a wider velocity profile, because of the cross-flow errors on the CTA instrumentation. Since the earlier hot-wire experiments do not conserve momentum, while our's do when corrected for the cross-flow errors, the narrower profiles of the earlier investigations must represent a problem with those experiments, and not with the technique used.

REFERENCES

1. Abbiss, J.B., J.S. Bradbury and M.P. Wright (1975) "Measurements on an Axisymmetric Jet Using a Photo Correlator, the Accuracy Flow Measurements by Laser Doppler Methods", Proc. LDA Symp, Copenhagen 319-335.

2. Buchhave, P. (1979) "The Measurement of Turbulence with the Burst Type LDA Errors and Correction Methods", Ph.D Dissertation, State University of New York at Buffalo.

3. Buchhave, P., W.K. George and J.L. Lumley (1979) "The Measurement of Turbulence with the LDA", Annual Review of Fluid Mech. 11, 443-503.

4. Capp. Steven P. (1983) "Experimental Investigation of the Turbulent Axisymmetric Jet" (1983) Ph.D Dissertation, State University of New York at Buffalo.

5. Corrsin, S. (1943), National Advisory Committee, Aeronaut. Wartime Reports No. 94.

6. Corrsin, S. and M.S. Uberoi (1949) National Advisory Committee, Aeronaut. Tech. Notes, 1865.

7. Corrsin, S. and M.S. Uberoi (1950) National Advisory Committee, Aeronaut. Tech. Notes, 2124.

8. Corrsin, S. and M.S. Uberoi (1950) "Further Experiments of the Flow and Heat Transfer in a Heated Turbulent Jet'', NACA Report 998.

9. George, W.K., Jr. (1979) "Processing of Random Signals", in Dynamics Measurements in Unsteady Flows, Proc. Dynamic Flow Conf. 1978, P.O. Box 121, DK 2740 Skovlunde, Denmark.

10. George, W.K., A.A. Seif and C.B. Baker (1982) "Momentum Balance Considerations in Axisymmetric Turbulent Jets", unpublished.

11. Hinze, J.D. and B.G. van der Hegge Zignen (1949) "Transfer of Heat and Matter in the Turbulent Mixing Zone of an Axially Symmetrical Jet", Applied Scientific Research, V A1, 435-461.

12. Hinze, J.D. (1975) "Turbulence", McGraw-Hill, New York, NY.

13. Khwaja, M.S. (1980) "Investigation of the Turbulent Axisymmetric Jet Mixing Layer", M.S. Thesis, State University of New York at Buffalo.

14. Nee, N. (1981) "Continuous Laser Doppler Anemometry Measurements in the Mixing Layer of an Axisymmetric Jet", M.S. Thesis, State University of New York at Buffalo.

15. Reichardt, H. (1942) "Gesetzma Bikeiten der freien turbrlenz" VDI-Forschungsheft, 4.4.

16. Reichardt, H. (1951) Forsch. Gebiete Ingenieurw., No. 414.

17. Rodi, W. (1975) "Method of Analyzing Hot-wire Signals in Highly Turbulent Flow and Its Evaluation in Round Jets. Disa Information No. 17.

18. Sami, S., T. Carmody and H. Rouse (1967) "Jet Diffusion in the Region of Flow Establishment", JFM, 27, 2, 231-252.

19. Seif, A.A. (1981) "Higher Order Closure Model for Turbulent Jets", Ph.D. Dissertation, State University of New York at Buffalo.

20. Townsend, A. A. (1956) "Turbulent Shear Flow", Cambridge University Press, Cambridge, England.

21. Tutu, N.K. and R. Chevray (1975) "Cross-wire Anemometry in High Intensity Turbulence'', JFM, 71, 785.

22. Wygnanski, I. and H. Fiedler (1969) "Some Measurements in the Self-Preserving Jet'', J. Fluid Mech. V.38, 3, 577-612.